

Answers to Anonymous Reviewer #1

“Near East Desertification: Impact of Dead Sea drying on convective rainfall” by Khodayar and Hoerner submitted to Atmospheric Chemistry and Physics

Dear Reviewer1:

Thanks for your comments and suggestions. We understand your point and we agree with it. We have modified the manuscript to better reflect the “story line”. In the following you can find a more detail answer to your comments (in blue).

Kind regards

Samiro Khodayar

I have read the author response to the comments. I understand there are limitations related to possibility to repeat simulations and availability of simulation data. But in the present state, the main message of this work, in my opinion, is basing on simulations that are not representing reality in few ways, that are already mentioned in my previous major comments (4 out of 5) and are summarized below (points 1 to 4 below).

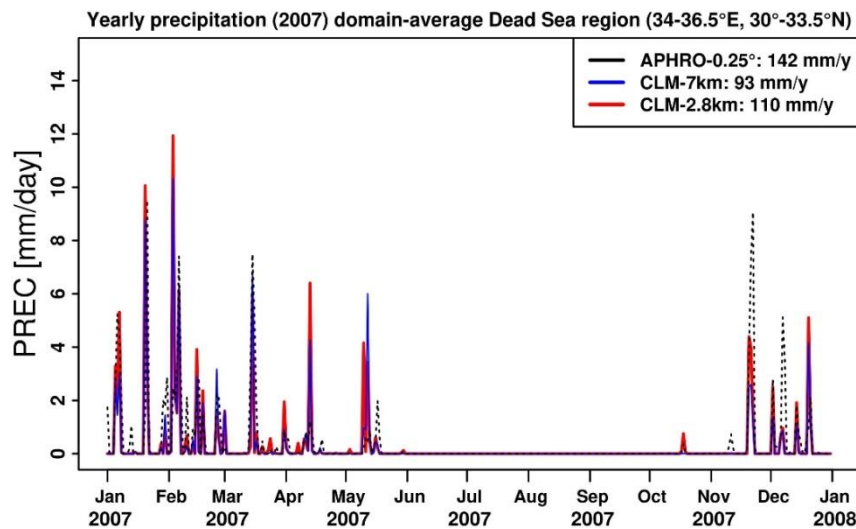
We understand and agree with the point of view and comments of the reviewer. We believe incorporating this point of view in the “story line” of the manuscript will improve it and make it clearer to the reader. Therefore, we have tried to better explain and clarify in every relevant part of the manuscript the fact that we are assuming certain aspects of the modelling exercise, which do not represent accurately reality. This is due to model and external input data limitations.

1) Precipitation totals are substantially underestimated by the REF simulation, especially on the shore but also in other regions. The authors show the same situation also when comparing to other datasets. They can further check it using stations from the Israeli Meteorological Service (IMS) which is freely available and includes many stations. Please see below the 1981-2010 mean annual rainfall from IMS (right) compared to the REF climatological run (left). My worry is that this underestimation may indicate a problem with the main moisture source for the precipitation in the Dead Sea. I am not clear how this discrepancy is handled. The authors refer to Rostkier-Edelstein 2014 paper, but in this work the fit with observations is much better and at the coast there is actually an overestimation of precipitation rather than underestimation.

In the first review, the reviewer1 and 2 asked us about these discrepancies in the precipitation field. As a consequence of this, we performed an intensive validation exercise with all adequate available data sets we could find at the time, EOBS suggested by the reviewer as well as *APHRODITE* data set suggested by experts in the area. The results show a general underestimation with particular focus on the near-coast flat areas and better results over the complex areas. We additionally performed new simulations demonstrating that neither the simulation domain, the forcing data or

the grid spacing used are the main reason for this bias. Indeed, closer results were obtained for the finer resolution simulations.

We additionally focused on particular periods, example 2007, common to all data sets and new simulations, and demonstrated that despite discrepancies in the mean spatial precipitation field, the comparison of the temporal evolution and the yearly sum for the particular periods quite well represented the precipitation events in the region.



In addition to that, the revision of past modelling investigations / literature in the region showed different biases in different models and resolutions. Some pointed out inaccuracies in the SST as the reason for the biases in the precipitation field in the Mediterranean coastal area, which is out of the scope of this paper to be demonstrated for our particular simulation.

We agree with the reviewer that these biases could affect the moisture sources for precipitation in the Dead Sea, however there are two relevant aspects to point out,

- The same bias is present in the ref and in the sen simulations; therefore, the bases for studying the sensitivity of HP in the region to modified conditions in the Dead sea (drying out the water) will be the same.
- The dominant wind conditions in the period and for the investigated cases are from the south, which reduces the possible impact of a dry bias on the north-western Mediterranean shore.

Nevertheless, we do agree with the reviewer that this is a relevant point to be discussed and further investigated. We have been able to identify several modelling aspects, which are not responsible of the biases present in the simulations of precipitation, namely, domain size, forcing data, grid spacing. We have included in the manuscript a discussion about the need to further investigate and correct this biases pointing out the possible impact on HP modelling in the region.

2) Lake evaporation: If I understood correctly, the lake evaporation is handled as regular sea water. But the Dead Sea is much more saline than sea water! Therefore, evaporation at the REF run should be lower than the simulated for regular sea.

The authors refer to Metzger et al. 2017 claiming that vapor pressure deficit being an important factor, rather than salinity, but exactly here salinity is considered, because saturated vapor pressure near the water is multiplied by the water activity that is reduced with salinity, and thus affecting the deficit. A good way to check the reference run would be to compare the simulated the annual lake evaporation with values published by Hamdani et al. (2018) [about 1130 mm/year for 2016-2017]. It seems that lake evaporation is computed, and is painted in magenta in Figure 5a, but this presents a range of 500-2000 mm/year, so it is hard to tell. I suggest to provide the annual lake evaporation and check how does it fit with observations. If it well fits, this is a very good indication for the model ability to represent this process, but otherwise, it would be a serious problem for the main claim of this study.

Yes, the model handles Dead Sea water as sea water. We already included in the previous version a comparison with observations as suggested by the reviewers

“Over the Dead Sea, the simulated average annual evaporation for the period under consideration is in the order of 1500-1800 mm/y, in contrast to the values in the deserts east and south, where the evaporation is less than 20 mm/y. Observed annual evaporation of this lake is known to be about 1500 mm, about 1130 mm/year for 2016-2017, and to vary with the salinity at the surface of the lake and freshening by the water inflow (Dayan and Morin 2006; Hamdani et al. 2018).”

3) The elevation of 405 and missing exposed steep slopes of the empty lake: I could not understand the authors reply. Yes, the lake area would be a bit smaller when is filled by soil, but not a lot, since the lake bottom is wide and the lake slopes are steep (e.g., Sirota et al., 2017). Yes, the bottom would not be at 720 mbsl (I did not claim it will) due to precipitation of NaCl, but surely not at 405 mbsl, which is already 25 m higher than present day lake level. I did not find an answer to why an elevation of 405 mbsl was selected and what about the exposed steep slopes and their potential effect on precipitation generation.

Again here we are limited by the ability of the model and the external data set to represent the reality of the region, and clearly this is the case. As described in the text, the shape, depth, soil types and characteristics of the Dead Sea itself and the region in general are imposed by the choice of external data sets, such as GLOBE from NOAA and HWSD from FAO in addition to the model grid spacing. We agree with the reviewer that a more realistic description of the area and conditions would be more advisable, we are trying to improve this point in our future simulations for the area, but it will also require future efforts in this direction.

4) Separating real effects from noise: the authors write in response to this comment that they obtained the same result in two different machines and that they “observe the same results in the 10-year long simulations and in the events simulated for several days, furthermore in many different events confirms that the effects presented in this paper are not random errors or noise”. I would appreciate showing this in more details. What do you mean – the same result in 10-years? do you get this pattern for each year separately? Also, the authors did not answer why we do not see the expected larger effect on the eastern side comparing to the western side.

We had two performed twice the same simulation in two different machines due to problems with the original machine in which the simulations were performed. To prove that not large differences were present in the different simulations due to the machine used we performed comparisons of some of the model outputs, e.g. the precipitation field. We did not find any significant deviation in our simulations. Unfortunately, because of storage capacity limitations we deleted the “old” simulations and the comparisons performed.

Regarding the sentence “*the fact that we observe the same results in the 10-year long simulations and in the events simulated for several days... confirms that the effects presented in this paper are not random errors or noise.*”, means that the same HPEs are simulated when performing the NWP simulations for short periods of days, than in the 10-year long simulations.

We could not give a definitive answer based on the information we have concerning the symmetrical differences on the west-east axis in Figure 5b (right), however, we believe the precipitation field itself shows also a symmetrical distribution, which has clearly an impact on the difference field, and the differences we are referring to are less than about 2-3 mm/y.

In summary – based on my understanding – at its present state, the paper shows:

Comparison of modeled precipitation in the Dead Sea region under two different hypothetical land use scenarios: 1) The Dead Sea is a lake with regular sea water, 2) The lake area is filled by soil to a level of 405 mbsl

Unless it is proved otherwise: scenario 1 is not representing the present conditions (points 1 and 2 above) and scenario 2 is not representing Dead Sea drying (point 3 above).

If this is the case, it is ok to leave the results as they are BUT the title, the “story” told in this paper, the objectives and the conclusions must be adjusted.

As mentioned before, we agree with the reviewer that certain assumptions have been made, which do not represent accurately the present or future reality. Therefore, we have accordingly modified the manuscript to clarify this point and the purpose of the manuscript to the reader.

We believe in most modelling realizations the limitations given and previously discussed will make very difficult to accurately represent the true conditions, although improvements could be applied. Moreover, although the topography and depth of the Dead Sea are not well represented in the model scenario, we have demonstrated that local conditions are sensible to the drying out of the lake. Therefore, we propose the following change in the title of the manuscript:

“Near East Desertification: sensitivity of the local conditions leading to convection to the Dead Sea drying out”

The objective of the paper has been defined as follows: *“the sensitivity of the local conditions to the drying out of the Sea is investigated focusing on the conditions leading to heavy precipitating convection in the region.”*

We included in the methodology and few sentences regarding the limitations of the model and the biases found for the reader to be aware of this issue *"We have to point out that the external data sets commonly employed describing relevant features of the Dead Sea region, such as the depth, shape and orography of the Dead Sea, as well as water characteristics at the reference run, do not accurately represent the reality. Also biases in relation to the precipitation field and evaporation over the Dead Sea have to be considered."*

Also we reflected in the conclusions this issue, for example in: *"Furthermore, a more realistic representation of the lake shape, water salinity and temperature, as well as Dead Sea abundance and depth must be addressed to more accurately describe present and expected future conditions. In the present study, limitations found in this direction in relation to model and external data set descriptions, as well as identified biases regarding for example moisture sources for HP in the region, MSB and Dead Sea evaporation, are expected to impact our results, and have to be improved in future efforts in the region. In a further step, the authors will investigate some of these issues in more detail,"*

Answers to Anonymous Reviewer #2

“Near East Desertification: Impact of Dead Sea drying on convective rainfall” by Khodayar and Hoerner submitted to Atmospheric Chemistry and Physics

Dear Reviewer2:

Thanks for your comments and suggestions. In the following you can find a more detail answer to your comments (in blue).

Kind regards

Samiro Khodayar

This is the 2nd round of reviews of the manuscript that presents an impact of Dead sea on the precipitation and evaporation in the surrounding areas. The authors have addressed satisfactorily my previous comments, but I still have a few specific comments. I list them below.

Specific comments:

1. Lines 51-54: Please reformulate the sentence. It is too long and is using “being” two times – sounds a bit strange.

“Since the Dead Sea is a terminal lake of the Dead Sea Valley, no natural outflow exists, evaporation is the main loss of water. The wind velocity and vapour pressure deficit are identified as the main governing factors of evaporation throughout the year (Metzger et al. 2017).”

2. Line 135: “... to have into...” -> “... to take into...”

Corrected

3. Line 160: “..., but with additional hourly output.”

Corrected

4. Line 161: This is a bit strange line, and I would omit it.

Corrected

5. Lines 163-168: You already write that in the previous section. Only once is enough... either here or in the previous section.

Thanks for the observation, we removed these lines here.

6. Lines 175-192: Although I would prefer that you show the evaluation of the simulation as a subsection in the results (or even as supplementary information), I find this part here a bit out of blue. It is too detailed and too long for something that you do not show, and this is still the methodology section. In addition, you only focus on the precipitation, but later in the results, you also look into other fields. I wonder if this can be summarized in a few lines, something like: “Comparison of the simulation with observations shows better/improved results at higher resolution, especially for precipitation, although some biases exist. These biases occur over... and could be related to...(refs)”

Following the reviewer’s advice we have shortened this part.

7. Lines 265-267: This is a bit strange line and I think it needs a reformulation in order to properly present what you did.

We have tried to improve this explanation.

8. Line 298: Decrease of 0.5 % is quite small, but this is (I assume) for mean precipitation. Maybe you should write then that this is for the mean precipitation, but you could also estimate that number for heavy precipitation.

We have indicated this value is in relation to the mean areal and temporal precipitation. To avoid misleading information we did not include a percentage for HP since this will be highly dependent on the season and/or type of events considered.

9. Lines 321-324: Note that these are now negative differences, so please carefully revise this part and all others where this change has an impact on the results.

Thanks for noticing, we have carefully read again the text and made the appropriate changes.

10: Table 1: Again, the event of 14.11 is missing. Instead, there is 15.11. Are these the same events and why are they marked differently in the table and in the text?

Thanks for noticing, this is just a mistake, the whole event covers the 14 to 15.11. We have corrected this information.

11. Line 1118: SEN(14.11) – This should be 19.11... the same as REF.

Corrected

12. Lines 1148-1149: Again, wrong REF and SEN... It should be 19.11 and not 14.11.

Corrected

13. Lines 1163-1164: The same as comment 11.

Corrected

14: Regarding the general comment 4 from a previous revision and replies to Reviewer 1: You should then also mention the spin-up period in the methodology... how you define it and if you discard some years from the analysis.

The spin-up time selection was already mentioned in L173-174.

Near East Desertification: sensitivity impact of Dead Sea drying on the local conditions leading to convection to the Dead Sea drying out

Samiro Khodayar^{1,2} and Johannes Hoerner²

¹Institute of Meteorology and Climate Research (IMK-TRO), Karlsruhe Institute of Technology (KIT), Karlsruhe, Germany

²Mediterranean Centre for Environmental Studies (CEAM), Valencia, Spain

Submitted to Atmospheric Chemistry and Physics
(HyMeX Inter-journal SI)

* Corresponding author. E-mail address: Khodayar_sam@gva.es (S. Khodayar)

Mediterranean Centre for Environmental Studies (CEAM),

Technological Park, Charles R. Darwin Street, 14 46980 - Paterna - Valencia - Spain

1 **Abstract**

2 The Dead Sea desertification-threatened region is affected by continual lake level
3 decline and occasional, but life-endangering flash-floods. Climate change has
4 aggravated such issues in the past decades. In this study, the impact on local
5 conditions impact of the Dead Sea drying leading to severe convection
6 generating heavy precipitation in the region of the drying out of the Dead Sea is
7 investigated. Sensitivity simulations with the high-resolution convection-permitting
8 regional climate model COSMO-CLM and several numerical weather prediction (NWP)
9 runs on an event time scale are performed over the Dead Sea area. A reference
10 simulation covering the 2003 to 2013 period and a twin sensitivity experiment, in which
11 the Dead Sea is dried out and set to bare soil, are compared. NWP simulations focus
12 on heavy precipitation events exhibiting relevant differences between the reference and
13 the sensitivity decadal realization to assess the impact on the underlying convection-
14 related processes.

15 The drying out of the Dead Sea is seen to affect the atmospheric conditions leading to
16 convection in two ways: (a) the local decrease in evaporation reduces moisture
17 availability in the lower boundary layer locally and in the neighbouring, directly affecting
18 atmospheric stability. Weaker updrafts characterize the drier and more stable
19 atmosphere of the simulations where the Dead Sea has been dried out. (b) Thermally
20 driven wind system circulations and resulting divergence/convergence fields are altered
21 preventing in many occasions convection initiation because of the omission of
22 convergence lines. On a decadal scale, the difference between the simulations
23 suggests that in future regional climate, under ongoing lake level decline, a
24 decrease in evaporation, higher air temperatures and less precipitation may be expected.

25

26

27

28

29

30

31 *Key Words: Dead Sea drying, climate change, convection, heavy precipitation,*
32 *boundary layer, wind systems, high-resolution modelling*

33 **1. Introduction**

34 The Eastern Mediterranean and the Middle East is a sensitive climate change area
35 (Smiatek et al. 2011). The anticipated warming in the 21st century combined with the
36 general drying tendency, suggest important regional impacts of climate change, which
37 should be investigated to assess and mitigate local effects on society and ecosystems.
38 The Dead Sea basin is dominated by semi-arid and arid climates except by the north-
39 western part that is governed by Mediterranean climate (Greenbaum et al. 2006). It is
40 an ideal area to study climate variation in the Near East. It was already discussed by
41 Ashbel (1939) the influence of the Dead Sea on the climate of its neighbouring regions.
42 The change in the climate of the Dead Sea basin caused by the drying of the Dead Sea
43 has also been evidenced in the last decades (Alpert et al. 1997; Cohen and Stanhill
44 1996; Stanhill 1994). The Dead Sea is the lowest body of water in the world (~ -430 m)
45 surrounded by the Judean Mountains (up to ~ 1 km amsl) to the west and to the east
46 by the Maob Mountains (up to ~ 3 km amsl). The area in between is rocky desert. The
47 complex topography of the area favours the combined occurrence of several wind
48 regimes in addition to the general synoptic systems, namely valley and slope winds,
49 Mediterranean breezes and local lake breezes (e.g. Shafir and Alpert 2011). These
50 wind systems are of great importance for the living conditions in the region since they
51 influence the visibility and the air quality (e.g. Kalthoff et al. 2000; Corsmeier et al.
52 2005) as well as the atmospheric temperature and humidity. Since the Dead Sea is a
53 terminal lake of the Dead Sea Valley, no natural outflow ~~exists,exists; being~~
54 evaporation is the main loss of water. ~~being~~ The wind velocity and vapour pressure
55 deficit are identified as the main governing factors of evaporation throughout the year
56 (Metzger et al. 2017). Through the high evaporation the lake level declines and results
57 in a desertification of the shoreline and a changing fraction of water and land surface in
58 the valley. The documented Dead Sea water level drop of about 1 m/y in the last
59 decades (Gavrieli et al. 2005) is mainly due to the massive water consumption at its
60 upstream having climate changes a small contribution to the lake level decrease
61 (Lensky and Dente 2015). This situation severely affects agriculture, industry and the
62 environmental conditions in the area, thus, leading to substantial economic losses
63 (Arkin and Gilat 2000).

64 The Jordan River catchment and Dead Sea-exhibit in the north, annual precipitation in
65 the order of 600-800 mm, whereas in the south, there is an all year arid climate with an
66 annual precipitation of <150 mm (Schaedler and Sasse 2006). Rain occurs between
67 October and May and can be localized or widespread (Dayan and Sharon 1980)
68 (Sharon and Kutiel 1986). Rainfall varies seasonally and annually, and it is often

69 concentrated in intense showers (Greenbaum et al. 2006) caused mainly by severe
70 convection (Dayan and Morin 2006). Flash floods are among the most dangerous
71 meteorological hazards affecting the Mediterranean countries (Llasat et al 2010), thus,
72 knowledge about the processes shaping these events is of high value. This is
73 particularly relevant in arid climates, where rainfall is scarce, and often, local and highly
74 variable. In flood-producing rainstorms, atmospheric processes often act in concert at
75 several scales. Synoptic-scale processes transport and redistribute the excess sensible
76 and latent heat accumulated over the region and subsynoptic scale processes
77 determine initiation of severe convection and the resulting spatio-temporal rainfall
78 characteristics. The main responsible synoptic weather patterns leading to heavy
79 rainfall in the region are in general well known and described in previous publications
80 (e.g. Belachsen et al. 2017; Dayan and Morin 2006). Belachsen et al. (2017) pointed
81 out that three main synoptic patterns are associated to these heavy rain events: Cyprus
82 low accounting for 30% of the events, Low to the east of the study region for 44%, and
83 Active Red Sea Trough for 26%. The first two originate from the Mediterranean Sea,
84 while the third is an extension of the Africa monsoon. Houze (2012) showed that
85 orographic effects lead to enhanced rainfall generation; rain cells are larger where
86 topography is higher. Sub-synoptic scale processes play a decisive role in deep
87 convection generation in the region. Convection generated by static instability seems to
88 play a more important role than synoptic-scale vertical motions (Dayan and Morin
89 2006). The moisture for developing intensive convection over the Dead Sea region can
90 be originated from the adjacent Mediterranean Sea (Alpert und Shay-EL 1994) and
91 from distant upwind sources (Dayan and Morin 2006).

92 | In this study, the sensitivity of the local conditions in the Dead Sea region to the drying
93 out of the ~~Dead~~-Sea is investigated focusing on the ~~impact on atmospheric~~-conditions
94 leading to heavy precipitating convection in the region. The relevance of the Dead Sea
95 as a local source of moisture for precipitating convection as well as the impact of the
96 energy balance partitioning changes and related processes caused by the drying of the
97 Dead Sea are investigated. With this purpose, a sensitivity experiment with the high-
98 resolution regional climate model COSMO-CLM [Consortium for Small scale Modelling
99 model (COSMO)-in Climate Mode (CLM); Böhm et al. 2006] is conducted. The high
100 horizontal grid spacing used (~ 2.8 km) resolves relevant orographic and small-scale
101 features of the Dead Sea basin, which is not the case when coarser resolution
102 simulations are performed. Moreover, at this resolution convection is explicitly resolved
103 instead of being parametrized, which has been already extensively demonstrated to be
104 highly beneficial for the simulation of heavy precipitation and convection-related

105 processes. The benefit of employing high-resolution convection permitting simulations
106 is mainly in sub-daily time-scales, (e.g., Prein et al., 2013; Fosser et al., 2014; Ban et
107 al., 2014), however, daily precipitation is also positively affected, particularly in winter
108 time (Fosser et al., 2014). Previous studies in the area applying high-resolution
109 modelling agree with the ~~beneficial~~beneficial impact of finer resolution against coarser
110 ones (e.g. *Rostkier-Edelstein et al. 2014; Hochman et al. 2018; Kunin et al. 2019*).

111 ~~The impact of completely drying the Dead Sea on the regional atmospheric conditions~~
112 ~~and precipitating convection is discussed.~~—A decadal simulation and several event-
113 based Numerical Weather Prediction (NWP) runs covering the eastern Mediterranean
114 are carried out. A process understanding methodology is applied to improve our
115 knowledge about how sub-synoptic scale processes leading to severe convection are
116 affected by the drying of the Dead Sea. The article is organized as follows. Section 2
117 provides an overview of the data and the methodology used. Then, in section 3, the
118 climatology of the region based on the high-resolution convection-permitting decadal
119 simulation is presented and the impact of drying out the Dead Sea is examined across
120 scales. Finally, conclusions are discussed in section 4.

121

122 **2. Data and methodology**

123 **2.1 The COSMO-CLM model**

124 In this investigation, the regional climate model (RCM) of the non-hydrostatic COSMO
125 model, COSMO-CLM (CCLM), is used (Version 5.0.1). It has been developed by the
126 Consortium for Small-scale modeling (COSMO) and the Climate Limited-area Modeling
127 Community (CLM) (Böhm et al., 2006). It uses a rotated geographical grid and a
128 terrain-following vertical coordinate. The model domain covers the southern half of the
129 Levant, centred around the Dead Sea, with a horizontal resolution of 7 km and 2.8 km,
130 60 vertical levels and a time step of 60 and 20 seconds, respectively. Using IFS
131 (Integrated Forecasting System) analysis, the spectral weather model of ECMWF
132 (European Centre for Medium-Range Weather Forecast) as driving data for the
133 simulations, a double nesting procedure was employed. The coarsest nest at 0.0625°
134 resolution (about 7 km) covers 250 grid points in x direction and 250 grid points in y
135 direction. The size and location of the 7 km domain has been considered large enough
136 to ~~have~~take into consideration all possible synoptic situations relevant for the
137 development of extreme phenomena in the study area as well as the influence of the
138 Mediterranean Sea. The finest nest at 0.025° (circa 2.8 km) covers 150 x 150 grid

139 points, thus a total area of 22500 grid points and includes the study area (72 grid point
140 in x direction and 92 in y direction) centred around the Dead Sea.

141 A Tiedtke (1989) mass-flux scheme is used for moist convection in the 7 km, and
142 reduced Tiedtke mass-flux scheme for shallow convection. Contrary to the CCLM-7 km
143 simulation, where convection is parameterized, in the CCLM-2.8 km convection is
144 explicitly resolved (Doms and Baldauf, 2015), so only the reduced Tiedtke mass-flux
145 scheme is used for shallow convection. The model physics includes a cloud physics
146 parameterization with 5 types of hydrometeors (water vapor, cloud water, precipitation
147 water, cloud ice, precipitation ice), a radiative transfer scheme based on a delta-two-
148 stream solution (Ritter and Geleyn, 1992) and a roughness-length dependent surface
149 flux formulation based on modified Businger relations (Businger et al., 1971).

150 Orography data from GLOBE (Global Land One-km Base Elevation Project) of NOAA
151 (National Oceanic and Atmospheric Administration) and soil data from HWSD
152 (Harmonized Worlds Soil Database) TERRA is used. HWSD is a global harmonization
153 of multiple regional soil data sets with a spatial resolution of 0.008° (FAO, 2009),
154 resulting in 9 different soil types in the model, namely 'ice and glacier', 'rock / lithosols',
155 'sand', 'sandy loam', 'loam', 'loamy clay', 'clay', 'histosols', and 'water'.

156 | Multiple model runs have been performed. A 7 km run from 2003 to 2013 with daily
157 output is used as nesting for two 2.8 km runs over the same time span. The Dead Sea
158 is dried out and replaced with soil types from the surrounding area in one of them
159 (SEN), the other one is used as reference (CLIM). For the detailed investigation of
160 convective events on 14.11.2011 and 19.11.2011, sub-seasonal simulations have been
161 performed with the same settings as the decadal simulation, but with additional hourly
162 outputs ~~due to the limitations imposed by the daily output.~~

163 **2.2 Methodology**

164 | ~~In order to assess the impact of the drying of the Dead Sea on the atmospheric~~
165 ~~conditions leading to severe convection in the region, a set of sensitivity experiments~~
166 ~~was performed.~~ A decadal simulation covering the 2003 to 2013 time period was
167 carried out with the convection permitting 2.8 km COSMO-CLM model. Lateral
168 boundary conditions and initial conditions are derived from the European Centre for
169 Medium-Range Weather Forecasts (ECMWF) data. The COSMO-CLM 7 km is used as
170 nesting step in between the forcing data and the 2.8 km run. This reference simulation
171 will be hereafter referred to as REF^{CLIM} simulation. Parallel to this, a sensitivity
172 experiment (hereafter SEN^{CLIM}) is carried out in which the Dead Sea is dried out and

173 set to bare soil on -405 m level (depth of the Dead Sea in the external data set, GLOBE
174 (Hastings and Dunbar, 1999)). After examination of the results, the first year of
175 simulations is considered spin-up time, thus, our analysis covers the 2004-2013 period.

176 The precipitation field has been validated using the EOBS dataset (resolution of 0.1°
177 and available for the period 1980-2011; Haylock et al. 2008) ~~with a resolution of 0.1°~~
178 ~~and available for the period 1980-2011~~, and the APHRODITE's (Asian Precipitation -
179 Highly-Resolved Observational Data Integration Towards Evaluation: Yatagai et al.
180 2008, 2012) daily gridded precipitation, ~~which is the only long-term continental-scale~~
181 ~~daily product that contains a dense network of daily rain-gauge data for Asia. It has a~~
182 resolution of 0.25° and ~~is~~ available for 1980-2007. The APHRODITE data shows
183 generalized lower precipitation values than EOBS, but still higher than our simulation
184 particularly close to the northern Mediterranean shoreline, over coastal-flat terrain,
185 whereas the best agreement is at areas dominated by complex terrain. ~~This agrees~~
186 ~~with previous high-resolution modelling activities in the region such as Restkier~~
187 ~~Edelstein et al. (2014) using WRF at 2 km. They suggest in this publication that~~
188 ~~inaccuracies in the gridded SST dataset used in the simulations could be responsible~~
189 ~~for the observed bias highlighting the strong sensitivity of precipitation in the~~
190 ~~Mediterranean basin to very small differences in the SST (Migliotta et al. 2011).~~
191 Despite these biases the comparison of the temporal areal-mean of the model
192 simulations at 7 km and 2.8 km and the APHRODITE dataset demonstrates that in
193 general the model quite quite well captures the precipitation events. An improvement
194 is seen at the finer resolution.

195 Regional dry and wet periods are identified and quantified in the simulations by means
196 of the Effective Drought Index (EDI; Byun and Wilhite 1999; Byun and Kim 2010). The
197 EDI is an intensive measure that considers daily water accumulations with a weighting
198 function for time passage normalizing accumulated precipitation. The values are
199 accumulated at different time scales and converted to standard deviations with respect
200 to the average values. Here we use an accumulation period of 365 days. EDI dry and
201 wet periods are categorized as follows: moderate dry periods $-1.5 < EDI < -1$, severe dry
202 periods $-2 < EDI < -1.5$, and extreme dry periods $EDI < -2$. Normal periods are revealed by
203 $-1 < EDI < 1$ values.

204 Based on daily mean values, precipitation and evapotranspiration distribution and
205 possible tendencies in the 10-year period are assessed. To further asses the most
206 affected areas in our study area, this is divided in four subdomains surrounding the
207 Dead Sea and trying to respect the orographic pattern in the area (Figure 3). Annual

208 cycles are thus separately investigated to take into consideration the relevant
209 differences in orography, soil types, and distance to the coast among others (Figure1),
210 which are known to have a significant impact in the precipitation distribution in the
211 region (e.g. Belachsen 2017; Houze 2012). . Differences in the annual cycle and
212 temporal evolution of precipitation and evapotranspiration between the REF^{CLIM} and
213 SEN^{CLIM} are discussed. Also, differences in the near-surface and boundary layer
214 conditions and geopotential height patterns are examined. Geographical patterns of
215 mean evapotranspiration and precipitation and differences with respect to the reference
216 simulation are assessed. Probability distribution functions (PDFs), and the Structure,
217 Amplitude and Location (SAL: Wernli et al. 2008) analysis methodologies are used to
218 illustrate differences in the mean and extreme precipitation between the reference and
219 the sensitivity experiments. The SAL is an object-based rainfall verification method.
220 This index provides a quality measure for the verification of quantitative precipitation
221 forecasts considering three relevant aspects of precipitation pattern: the structure (S),
222 the amplitude (A), and the location (L). The A component measures the relative
223 deviation of the domain-averaged rainfall; positive values indicate an overestimation of
224 total precipitation, negative values an underestimation. The component L measures the
225 distance of the center of mass of precipitation from the modelled one, and the average
226 distance of each object from the center of mass. The component S is constructed in
227 such a way that positive values occur if precipitation objects are too large and/or too
228 flat and negative values if the objects are too small and/or too peaked, quantifying the
229 physical distance between the centres of mass of the two rainfall fields to be compared.
230 Perfect agreement between prediction and reference are characterized by zero values
231 for all components of SAL. Values for the amplitude and structure are in the range (-2,
232 2), where ± 0.66 represents a factor of 2 error. The location component ranges from 0
233 to 2, where larger values indicate a greater separation between centres of mass of the
234 two rainfall fields. This is done by selecting a threshold value of 1/15 of the maximum
235 rainfall accumulation in the domain (following Wernli et al. 2008). The structure and
236 location components are thus independent of the total rainfall in the domain.

237

238 Differences in the temporal evolution of precipitation between the REF^{CLIM} and SEN^{CLIM}
239 are identified. In Table 1, those events in which an area-mean (study area, Figure 1)
240 difference between both simulations higher than ± 0.1 mm/d exists are selected as
241 potential heavy precipitation events and classified attending to their synoptic scale
242 ~~environment,environment~~ and atmospheric stability conditions (Table 1).

243 Although Dayan and Morin (2006) discuss that in general large-scale vertical motions
244 do not provide the sufficient lifting necessary to initiate convection, it was demonstrated
245 by Dayan and Sharon (1980) that a relationship exists between the synoptic-scale
246 weather systems and deep moist convection, being those systems responsible for the
247 moisturizing and destabilization of the atmosphere prior to convective initiation. They
248 pointed out that indices of instability proved the most efficient determinants of the
249 environment characterizing each rainfall type in the region. Thus, two indicators of the
250 atmospheric degree of stability/instability, namely the Convective Available Potential
251 Energy (CAPE; Moncrieff and Miller 1976) and the KO-index (Andersson et al. 1989),
252 are examined in this study. The CAPE is a widely known index indicating the degree of
253 conditional instability. Whereas, the KO-index, which is estimated based on the
254 equivalent potential temperature at 500, 700, 850 and 1000 hPa (following the
255 recommendations by Bolton 1980), describes the potential of deep convection to occur
256 as a consequence of large-scale forcing (Andersson et al. 1989; Khodayar et al. 2013).
257 Generally, regions with KO-index < 2 K and large-scale lifting are identified as
258 favourable for deep convection. Parcel theory (50 hPa ML (Mixed Layer) parcel) and
259 virtual temperature correction (Doswell and Rasmussen 1994) are applied to these
260 calculations.

261 Based on the above criteria, a separation was made between events with widespread
262 rainfall and those more localized. Among the latter, we selected two events to illustrate
263 the local impacts on the boundary layer conducive to deep moist convection.
264 Particularly, differences in the amount, structure and location of precipitation are
265 assessed by examining the spatial patterns and the SAL verification method. The two
266 selected events for detail analysis in this study are those showing the larger SAL
267 deviations. Those two cases occur close in time, but they are not the same event. No
268 differences in the soil and atmospheric conditions have been found in the period
269 between the events when the REF and SEN simulations are compared. Carefull
270 inspection of the atmospheric conditions after the first event shows no significant
271 differences between simulations suggesting no connotion between both events. Even
272 though a more detail analysis is provided for the two selected cases, all convective-
273 events listed in Table 1 have been examined to assess the main impacts on the
274 mechanisms leading to convection. High-resolution simulations with the NWP COSMO
275 2.8 km model are performed with hourly output temporal resolution and covering a 3-
276 day period (including 48-h prior to the day of the event, from 00 UTC) to capture
277 atmospheric pre-conditions conducive to deep moist convection. For this, a reference

278 simulation, REF^{NWP}, and a sensitivity experiment, SEN^{NWP}, are carried out for each
279 event.

280 We have to point out that the external data sets commonly employed describing
281 relevant features of the Dead Sea region, such as the depth, shape and orography of
282 the Dead Sea, as well as Dead Sea water characteristics at the reference run, do not
283 accurately represent the reality. In the same direction, biases in relation to different
284 variables such as the precipitation field and evaporation over the Dead Sea have to be
285 considered.

286

287

288 3. Results and discussion

289 3.1 Climatology of the Dead Sea region

290 *Annual cycle*

291 To assess the climatology of the study region (Figure 1) the annual evaporation and
292 precipitation cycles based on daily means of the respective quantities are investigated
293 (Figure 2). Additionally, we examine the evolution of specific humidity ($Q_{v_{2m}}$) and
294 temperature at 2 m (T_{2m}) as well as total column integrated water vapour (IWV) and
295 low-boundary layer (< 900 hPa) equivalent potential temperature (Θ_e). Possible
296 changes in the atmospheric stability conditions are evaluated by examination of the
297 CAPE and KO-index. In Figure 2, all grid points over the study region (Figure 1) and
298 the time period 2004-2013 are considered. Differences between the REF^{CLIM} and the
299 SEN^{CLIM} simulations are also discussed.

300 The annual cycle of evaporation shows minimum values in the autumn season (around
301 October, ~ 0.1 mm/d) and maximum evaporation in spring (around March, ~ 0.4 mm/d).
302 The dependency with the precipitation cycle is clear with maximum values of the latter
303 around March and rain occurring between October and May (Figure 2a) in agreement
304 with observations in the area (Dayan and Sharon 1980). The difference between the
305 evaporation in the REF^{CLIM} and the SEN^{CLIM} simulations indicates a mean decrease in
306 the order of 0.02 (February) to ~ 0.1 (August) mm/d in the absence of the Dead Sea
307 water (SEN^{CLIM}). The largest difference is in the dry period (May to October) when
308 water availability is less dependent on precipitation, and evaporation is higher over the
309 Dead Sea in contrast to the minimum values over land (Metzger et al. 2017). In
310 general, there is a decrease of about 0.5 % in mean precipitation in the SEN^{CLIM}

311 simulation. In contrast to the differences in evaporation, precipitation differences
312 between the reference and the sensitivity experiment occur in both directions during
313 the rain period, from October to May. Examining the total number over the whole
314 decadal simulation it is seen that the number of dry or wet days (> 0.1 mm/d) or heavy
315 precipitation events is not largely affected in the sensitivity experiment. In general, the
316 number of dry days increases (fewer wet days) in the SEN^{CLIM} simulation, whereas the
317 number of high intensity events show almost no variation. For each simulation, the
318 difference between precipitation and evaporation is negative mainly in spring and
319 summer contributing to the dryness in the region. Furthermore, the ~~negative~~ difference
320 between the REF^{CLIM} and SEN^{CLIM} simulations indicates that ~~the~~ PREC-EVAP
321 ~~difference~~ is higher in the SEN^{CLIM} simulation probably in relation to the reduced
322 evaporation over the dry sea area and the general decrease in the precipitation amount
323 in the region.

324 In addition to the reduced evaporation and precipitation (about 0.5 %) in the whole
325 domain in the SEN^{CLIM} simulation a drier and warmer lower-troposphere is identified
326 (Figure 2b) in agreement with the observational assessment by Metzger et al. (2017) of
327 the cooling effect of evaporation on air temperature in the region. The annual cycle of
328 IWV and $\Theta_{e<900\text{hPa}}$ in Figure 2c show that the impact of the dry Dead Sea resulting
329 evaporation is less pronounced when a deeper atmospheric layer is considered.
330 Indeed, $\Theta_{e<900\text{hPa}}$ evolution evidences that the warming effect due to the decreased
331 evaporation in the SEN^{CLIM} simulation is restricted to the near surface.

332 In Figure 2d, the annual cycle of areal mean CAPE displays larger values in the period
333 from August to November, being this the period more favourable for convection.
334 ~~Positive-Negative~~ CAPE differences between the REF^{CLIM} and the SEN^{CLIM} simulations
335 are presumably in relation to the identified distinct lower-atmospheric conditions, being
336 these more favourable and consequently CAPE values higher in the REF^{CLIM}
337 simulation. In the same period, the KO-index indicates a more potentially unstable
338 atmosphere, i.e. prone to deep convection because of large-scale forcing, and larger
339 differences between simulations.

340 In agreement with the well-known precipitation distribution in the region most of the
341 events occur in A1 (north-west) and A2 (north-east). Also, in these subdomains larger
342 differences between the REF^{CLIM} and SEN^{CLIM} simulations are identified pointing out the
343 relevance of the Dead Sea evaporation in the pre-convective environment for rainfall
344 episodes over the study area (Figure3a). Considering only land grid points almost no
345 difference between simulations is found in the evaporation annual cycle of A1 and A2

346 (Figure3b) suggesting the distinct amount of moisture advected towards A1 and A2
347 from the Dead Sea in REF^{CLIM} and SEN^{CLIM} as responsible for the differences in the
348 boundary layer conditions conducive to convection. Also, in these subdomains the
349 dryer and warmer lower boundary layer and the reduced instability in the SEN^{CLIM} are
350 recognized

351 *Inter-annual variability*

352 In Figures 4 we discuss the inter-annual variability (based on monthly-daily areal mean
353 values) of evaporation, precipitation as well as drought evolution.

354 The reduced evaporation in the annual cycle of the SEN^{CLIM} simulation for the whole
355 investigation domain, resulting from the drying of the Dead Sea and affected
356 evaporation, remains from year to year (Figure 4a). Larger differences between the
357 simulations occur in the May to November months in agreement with the annual cycle
358 in Figure 2a. This, and the time period of the maximum/minimum is constant over the
359 years. A tendency towards lower evaporation at each simulation and higher differences
360 between both at the end of the period are identified. An inter-annual fluctuation is
361 observed in both REF^{CLIM} and SEN^{CLIM} simulations. The yearly rate of evaporation
362 shows, for example, in REF^{CLIM} maximum values of about 7 mm in 2011 and around 17
363 mm in 2012. This is in agreement with the positive correlation expected between
364 precipitation and evaporation, a trend towards decreased precipitation and a
365 correspondence between drier years such as the 2011-2012 period and lower annual
366 evaporation are seen in Figure 4b. Year to year EDI calculations in Figure 4c help us
367 identify the regional extreme dry and wet periods. The EDI range of variation from
368 about -1 to 2 for the whole period of simulation indicates that the dry condition is the
369 common environment in the area, while the wet periods, EDI up to 6, could be
370 identified as extreme wet periods (relative to the area), in this case in the form of heavy
371 precipitation events. Maximum positive EDI values are in the first months of the year in
372 agreement with the precipitation annual cycle in Figure 2, whereas minimal EDI values
373 occur in summer and autumn indicative of the dry conditions in these periods.
374 Differences in the EDI calculations from both simulations reveal distinct precipitation
375 evolutions and denote timing differences in the occurrence of the precipitation events.
376 When the regional climate evolution is examined in combination with the impact on the
377 number of heavy precipitation events (Table 1) the impact is stronger in the dry period
378 of 2011 (Figure 4a). About six events show relevant differences in this period, contrary
379 to the average 3 episodes per year.

380 *Spatial distribution*

381 The geographical patterns of evaporation and precipitation are presented in Figure 5.
382 Over the Dead Sea, the simulated average annual evaporation for the period under
383 consideration is in the order of 1500-1800 mm/y, in contrast to the values in the deserts
384 east and south, where the evaporation is less than 20 mm/y. Observed annual
385 evaporation of this lake is known to be about 1500 mm and to vary with the salinity at
386 the surface of the lake and freshening by the water inflow (Dayan and Morin 2006;
387 Hamdani et al. 2018). Over land, higher evaporation is seen over the Judean
388 Mountains and the Jordanian Highlands. High correlation with the orography and soil
389 types is seen (Figure 1). Evaporation is probably correlated with rainfall which in turn is
390 correlated with topography. Particularly, in the Jordanian Highlands where maximum
391 evaporation is around 200 mm/y, the complex topography coincides with sandy loam
392 soils, whereas most of the soil in study region is defined as loamy clay or clay (Figure
393 1). The evaporative difference field between simulations in Figure 5a shows a highly
394 inhomogeneous patchiness not evidencing any relationship with orography or soil type,
395 but rather with changes in the precipitation pattern in the SEN^{CLIM} simulation as seen in
396 Figure 5b.

397 In agreement with the temporal series of areal mean precipitation in Figure 3 higher
398 annual precipitation are in the north-west and -east, with respect to the southern
399 regions. Topographic features exert a large impact on precipitation distribution with
400 maxima of about 175 to 300 mm/y over the Judean Mountains and the Jordanian
401 Highlands. To the northern end of the Dead Sea valley, the largest precipitation
402 difference between the REF^{CLIM} and the SEN^{CLIM} simulations is identified, rather than
403 directly over the Dead Sea area noting the importance of advected moisture from the
404 Dead Sea evaporative flux upslope and along the Dead Sea valley as well as the
405 indirect effects of a different spatial distribution of low-tropospheric water vapour in the
406 occurrence of precipitating convection.

407 Regarding the impact on the large-scale conditions, differences in the spatial pattern
408 and strength of the 500 hPa geopotential height field are identified over the Dead Sea
409 (not shown). In the 10-year mean, differences up to 0.002gpdm higher in SEN than in
410 REF are observed. Around the Dead Sea area, the differences are smaller and more
411 irregular. Generally, the differences are higher in the east of the Dead Sea than in the
412 west.

413 *Precipitation probability distribution function*

414 While the probability for lower intensity precipitation is very similar in the REF^{CLIM} and
415 the SEN^{CLIM} simulations differences are recognized in the higher precipitation

416 intensities, from about 150 mm/d (Figure 6a). Particularly, above 180 mm/d extreme
417 precipitation values occur less frequent at the SEN^{CLIM} simulation where a drier,
418 warmer and more stable atmosphere is identified (Figure 2).

419 *SAL*

420 The use of the SAL method in this study differs from the approach frequently presented
421 in literature since it is here not our purpose to examine differences between the
422 simulated field and observations (adequate observations for this comparison are not
423 available in the area), but to compare changes regarding the structure, amount and
424 location of the precipitation field between our reference and sensitivity experiments.
425 Figure 6b shows that when the mean precipitation over the whole simulation period is
426 considered all three SAL components are close to zero, meaning that very small
427 differences are found. However, when single precipitation events in the REF^{CLIM}
428 simulation are compared with the same period at the SEN^{CLIM} simulation, larger
429 differences regarding structure, amount and location of rainfall events are found. For
430 further examination of this issue two exemplary heavy precipitation events (indicated by
431 boxes in Figure 6b) are analysed in detail. In both cases, a negative A-component is
432 recognized, that is, less precipitation falls in the SEN^{CLIM} simulation. The S-component
433 also evidences the change in the structure of the convective cells. The L-component is
434 low meaning that the convective location does not change significantly in the SEN^{CLIM}
435 simulation, in contrast to the intensity and structure of the cells.

436

437 **3.2 Sensitivity of atmospheric conditions to the Dead Sea drying: episodic** 438 **investigation**

439 Among those events exhibiting differences in the precipitation field between both
440 simulations (Table 1 and Figure 6b) two situations occurring in the time period of the 14
441 to 19 November 2011 are investigated in the following.

442 In this term, the synoptic situation is characterized by a Cyprus low and its frontal
443 system located over the Dead Sea at about 00 UTC on the 15 November 2011 and at
444 12 UTC on the 18 November 2011. The low-pressure system and its frontal system
445 induced strong south-westerly to westerly winds with mean wind velocities up to 15
446 m/s.

447 In the first situation (hereafter CASE1), in association with the western movement of
448 the cold front a convective system develops over the Jordanian Highlands with

449 precipitation starting at about 21 UTC on the 14 November 2011. This convective
450 system is of high interest because of the large difference in its development between
451 the REF^{14.11} and the SEN^{14.11} simulations.

452 In Figure 7a the 24-h accumulated precipitation, from 14.11 09 UTC to 15.11 08 UTC,
453 in the investigation area is shown for the REF^{14.11} and the SEN^{14.11} simulations. Two
454 precipitation areas are seen, on the north-western and north-eastern of the Dead Sea.
455 Larger difference between models is on the north-eastern region (24-h accumulated
456 precipitation > 100 mm/d in REF^{14.11}, while < 50 mm/d in SEN^{14.11}), which is the focus of
457 our analysis.

458

459 The REF^{14.11} simulation shows that in the 6 hours period prior to the initiation of
460 convection the pre-convective atmosphere and more specifically the lower boundary
461 layer exhibit a moist (IWV ~ 24-30 mm, qvPBLmax ~ 7-10 g/kg) and unstable (CAPE ~
462 1100 J/kg; KO-index ~ -8 K; not shown) air mass on the western side of the
463 investigation area, particularly close to the western Mediterranean coast, and drier
464 (IWV~ 8-16; qvPBLmax ~ 4-6 g/kg) and more stable conditions (CAPE< 200 J/kg; KO-
465 index ~ 0-2 K) on the eastern side of the domain (Figure 7b). A maximum difference of
466 about 5 g/kg from west to east is established in the lower boundary layer.

467 Main differences between both simulations are over the Dead Sea (IWV difference up
468 to 2 mm and qvPBL up to 1.5 g/kg) and north and north-east of it, but almost similar
469 conditions everywhere else. In our target area (subdomain of investigation where the
470 convection episode takes place (red box in Figure 7)), north-east of the Dead Sea, a
471 drier and a more stable atmosphere is identified at the SEN^{14.11} simulation.

472 The evolution of the wind circulation systems in the area is similar in both simulations
473 (Figure 7c). The 700 hPa, 850 and 950 hPa winds dominantly blow from the south
474 south-west during the pre-convective environment advecting the moist unstable air
475 mass towards the Dead Sea valley and north-east of it, directly affecting the
476 atmospheric conditions at the target area (for a comparison with a climatology of the
477 wind conditions in the region please see Metzger et al. 2017). In both simulations, the
478 passage of the cold front over the Dead Sea establishes a strong southerly wind from
479 about 10 UTC on the 14 November 2011.

480 Prior to this time, dry air was advected below about 850 hPa towards the target area
481 from the east. The turning of the low-level winds and the resulting moistening of the
482 atmosphere is well and equally captured by both simulations (Figure 8a). Furthermore,
483 at the near-surface, from about 16 UTC, ~ 5 h prior to convection initiation in the target
484 area, a near-surface convergence line forms at the foothills of the northern part of the

485 Jordanian Highlands, which is also well and equally captured by both simulations
486 (Figure 8b). The lifting provided by the convergence line triggers convection in the
487 area. However, the drier and more stable atmosphere in the SEN^{14,11} simulation results
488 in less intense convection, weaker updrafts, and reduced precipitation at the eastern
489 slope of the valley.

490

491 In the second case, CASE2, we address an episode of localized convection taking
492 place on the north-western edge of the Dead Sea in the REF simulation, whereas no
493 convection develops in the SEN simulation. The isolated convection in the REF
494 simulation left about 50 mm rain in 3 h starting at about 03 UTC on the 19 November
495 2011 (Figure 9).

496 In contrast to CASE1, the modification of the pre-convective environment relevant for
497 convective initiation is in this case dominated by dynamical changes in the mesoscale
498 circulations. Differences in the evolution and strength of the Mediterranean Sea Breeze
499 (MSB), the Dead Sea breeze and orographic winds influence atmospheric conditions in
500 the target area leading to the assistance to or to the absence of convection. The most
501 significant difference observed between the simulations is in the development of a
502 strong near-surface convergence line in the REF simulation (which is not present in the
503 SEN simulation hindering convection in the area), which forms about 2 h before
504 convective initiation (Figure 10).

505 Even in the first hours of the 18 November 2011 differences in the speed and direction
506 of the near-surface winds over the Dead Sea and on the eastern flank of the Jordanian
507 Highlands could be identified. A fundamental difference between simulations occurs
508 from about 17 UTC when strong westerly winds indicating the arrival of the MSB reach
509 the western shore of the Dead Sea. One hour later, in the REF^{19,11} run the MSB
510 strongly penetrates the Dead Sea valley reaching as far as the eastern coast in the
511 centre to south areas. However, in the SEN^{19,11} simulation the MSB does not penetrate
512 downward, instead strong northerly winds flow along the valley (Figure 10a). Numerous
513 observational and numerical studies carried out to investigate the dynamics of the MSB
514 (e.g. Naor et al. 2017; Vuellers et al. 2018) showed that the downward penetration of
515 the MSB results from temperature differences between the valley air mass, which is
516 warmer than the maritime air mass. An examination of temperature differences along a
517 near-surface north-south valley transect (positions in Figure 10a) indicates a decrease
518 of about 4 °C at the near-surface over the dried Dead Sea area in contrast to negligible
519 changes on a parallel transect inland, on the western coast of the Dead Sea. These

520 evidences the notorious impact of the absence of water in the valley temperature, thus,
521 gradients in the region. The colder valley temperatures do not favour the downward
522 penetration of the MSB, which strongly affects the atmospheric conditions in the valley.
523 Moreover, a north-easterly land breeze is visible from about 20 UTC on the eastern
524 shore of the Dead Sea in the REF^{19,11} simulation, but not in the SEN^{19,11} simulation
525 (Figure 10b). This situation reflects an interesting case different from the ones
526 generally presented in former investigations in the area (e.g. Alpert et al. 1997 ; and
527 Alpert et al. 2006b) in which due to the recent weakening of the Dead-Sea breeze,
528 mainly because of the drying and shrinking of the Sea, the Mediterranean breeze
529 penetrates stronger and earlier into the Dead-Sea Valley increasing the evaporation
530 because of the strong, hot and dry wind.

531 Mountain downslope winds develop in both simulations from about 22 UTC. One hour
532 later, strong northerly valley flow in the northern part of the Dead Sea contrasts with the
533 westerly flow in the SEN^{19,11} simulation (Figure 10c). As the valley cools down during
534 night time in the SEN simulation, T2m decreases about 1 K from 20 UTC to 03 UTC in
535 contrast with the 0.1 K decrease of the Dead Sea in the REF simulation, the
536 temperature gradient weakens and the northerly valley flow present in the REF
537 simulation is absent in the SEN simulation. During the night, the synoptic conditions
538 gain more influence than the local wind systems governing the conditions in the valley
539 during day time. South-easterly winds prevail in the valley in both simulations. Much
540 stronger wind velocities are reached in the REF simulation, confirming the sensitivity of
541 large-scale dynamics to near-surface climate change-induced impacts.

542 The encounter of the north north-westerly and south south-easterly winds over the
543 Dead Sea area in the REF^{19,11} simulation induces the formation of a convergence zone,
544 which intensifies and extends offshore over the next hours and determines the location
545 of convective initiation. Meanwhile, homogeneous south-easterly winds are observed in
546 the SEN simulation (Figure 10d).

547 The differences in the wind circulations contribute to a different distribution of the
548 atmospheric conditions in the target area, particularly, low-tropospheric water vapour
549 as seen in the vertical cross sections in Figure 11. The evolution of the atmospheric
550 conditions in the 3-h period prior to convective initiation evidences the deeper and
551 wetter boundary layer in the REF^{19,11} simulation at the north-western foothills of the
552 ridge at the Jordanian Highlands. Differences of IWV up to 2 mm, and of instability
553 (CAPE) close to 200 J/kg are found in this area (not shown). This is the location of the
554 convergence line where convective updrafts, which start close to the ground, are

555 triggered reaching a maximum vertical velocity of about 5 m/s above the convergence
556 zone in the REF^{19,11} simulation.

557

558 **4. Conclusions**

559 The drying and shrinking of the Dead Sea has been extensively investigated in the last
560 decades from different points of view. This process has been related to significant local
561 climate changes which affect the Dead Sea valley and neighboring regions. The
562 climate of the Dead Sea is very hot and dry. But occasionally the Dead Sea basin is
563 affected by severe convection generating heavy precipitation, which could lead to
564 devastating flash floods.

565 In this study, high-resolution COSMO model simulations are used to assess the
566 ~~sensitivity-impact~~ of ~~the~~ Dead Sea changes on the occurrence of convective
567 precipitation in the region. A set of high-resolution, ~ 2.8 km, climate simulations
568 covering the period 2003 to 2013, and several numerical weather prediction (NWP)
569 runs on an event time scale (~ 48-36 h) are performed over the Dead Sea area. On a
570 decadal time scale, two simulations are carried out. The first “reference” run with the
571 Dead Sea area, and a second run “sensitivity” in which the Dead Sea is dried out and
572 set to bare soil. The NWP simulations focus on two heavy precipitation events
573 exhibiting relevant differences between the reference and the sensitivity decadal runs.
574 A total of four simulations are performed in this case.

575 As the energy balance partitioning of the Earth’s surface changes due to the drying of
576 the Dead Sea, relevant impacts could be identified in the region. From a climatological
577 point of view, ~~in a future regional climate under ongoing~~ the drying out of the Dead Sea
578 ~~results in level decline,~~ less evaporation, higher air temperatures and less precipitation
579 ~~is to expect.~~ Reduced evaporation over the Dead Sea occurs from May to October. The
580 cooling effect of evaporation in the neighboring areas results in an increase of T-2m ~~in~~
581 ~~the absence of the Dead Sea.~~ Atmospheric conditions, such as air temperature and
582 humidity, are mostly affected in the lower-tropospheric levels, which in turn influence
583 atmospheric stability conditions, hence, precipitating convection. In general, the
584 number of dry/wet days is not largely affected by the drying out of the Dead Sea,
585 although these differences could be larger for hourly precipitation; rather the structure
586 and intensity of the heavier precipitation events is changed. While a general and
587 homogeneous decrease in evaporation is seen at the SEN^{CLIM} simulation, precipitation
588 deviations occur in both directions, which could suggest and impact on the timing of the

589 events. A relevant year to year variability is observed in evaporation-precipitation which
590 indicates the need of long time series of observations to understand local conditions
591 and to validate model simulations.

592 The detailed analysis of two heavy precipitation events allowed us to further assess the
593 possible causes and the processes involved regarding the decrease in precipitation
594 intensity or the total omission of convection with respect to the reference simulation in
595 the absence of the Dead Sea water. Two main components, strongly affected by the
596 drying out of the Dead Sea, are found to be highly relevant for the understanding of the
597 environmental processes in the Dead Sea region.

598 (a) First, the lower-atmospheric boundary layer conditions. Changes in the energy
599 balance affect the atmosphere through the heat exchange and moisture supply. The
600 drying of the Dead Sea in the SEN simulations and the resulting decrease in local
601 evaporation, impact the Dead Sea Basin conditions and the neighbouring areas. A
602 reduction in boundary layer humidity and an increase in temperature result in a general
603 decrease of atmospheric instability and weaker updrafts indicating reduced deep-
604 convective activity. Main differences on the atmospheric conditions are directly over the
605 Dead Sea, but these conditions are frequently advected to neighbouring areas by the
606 thermally driven wind systems in the region which play a key role for the redistribution
607 of these conditions and the initiation of convection.

608 (b) Secondly, wind systems in the valley. In the arid region of the Dead Sea Basin with
609 varied topography, thermally and dynamically driven wind systems are key features of
610 the local climate. Three different scales of climatic phenomena coexist: The
611 Mediterranean Sea Breeze (MSB), the Dead Sea breeze and the orographic winds,
612 valley-, and slope-winds, which are known to temper the climate in the Dead Sea valley
613 (Shafir and Alpert, 2011). The drying of the Dead Sea in the SEN simulation disturbs
614 the Dead Sea thermally driven wind circulations. The Dead Sea breezes are missing,
615 weaker wind speeds characterize the region and along valley winds are consequently
616 affected. Furthermore, the dynamics of the Mediterranean breeze penetration into the
617 Jordan Valley are affected.

618

619 Consequently, the impacts on convection initiation and development are twofold:

620 (i) Distinct redistribution of atmospheric conditions, locally or remotely, which yields to
621 different atmospheric conditions that in the absence of the Dead Sea result in a
622 reduced moisture availability in the lower atmospheric levels and increased stability
623 hindering convection or reducing the intensity of the events.

624 (ii) Modification of the divergence/convergence field. The absence of the Dead Sea
625 substantially modifies the wind circulation systems over the Dead Sea valley, which
626 leads to the omission of convergence lines which act as triggering mechanism for
627 convection.

628

629 We can conclude that in general the lack of sufficient low-atmospheric moisture in
630 relation to the drying out of the Dead Sea, the increase of atmospheric stability in
631 addition to an absence or reduction in the intensity of the convergence zones, works
632 against initiation or intensification of precipitating convection in the area. The relevance
633 of the small-scale variability of moisture and the correct definition and location of
634 convergence lines for an accurate representation of convective initiation illustrates the
635 limitation and the lack of adequate observational networks in the area and the need for
636 high-resolution model simulations of boundary layer processes to predict intense and
637 localised convection in the region.

638 These results contribute to gain a better understanding of ~~expected the sensitivity of~~
639 local conditions in the Dead Sea valley and neighbouring areas ~~under to continual~~ lake
640 level decline. Energy balance partitioning and wind circulation systems are determinant
641 for local climatic conditions, e.g. temperature and humidity fields as well as aerosol
642 redistribution, therefore, any change should be well understood and properly
643 represented in model simulations of the region. Our results point out, in agreement with
644 past modelling activities in the region, the need to further improve the representation of
645 precipitation fields in the area, particularly close to the Mediterranean coastline. More
646 accurate Mediterranean SST input fields have been suggested as relevant to reduce
647 the model inaccuracies. Furthermore, a more realistic representation of the lake shape,
648 water salinity and temperature, as well as Dead Sea abundance and depth must be
649 addressed to more accurately describe present and expected future conditions. In the
650 present study, limitations found in this direction in relation to model and external data
651 set descriptions, as well as identified biases regarding for example moisture sources
652 for HP in the region, MSB and Dead Sea evaporation, are expected to impact our
653 results, and have to be improved in future efforts in the region. the impact on the
654 simulation results. In a further step, the authors will investigate some of these issues
655 performing sensitivity experiments in more detail, and will assess the impact of model
656 grid resolution on the horizontal and vertical flow field in the region across scales,
657 including the impact on large-scale dynamics. We will also put emphasis in trying to
658 better understand the dynamics of the MSB under lake level decline using high-
659 resolution modelling, especially the contrasting behaviour pointed out in this study. Fine

660 resolution simulations up to 100 m will be performed for this purpose. Furthermore, we
661 will provide a verification of the complex chain of processes in the area using unique
662 measurements in the framework of the interdisciplinary virtual institute Dead Sea
663 Research VEnue (DESERVE; Kottmeier et al., 2016).

664

665 **Author contribution**

666 SK wrote the manuscript, analysed the data, interpreted the results and supervised the
667 work. JH carried out data analysis, interpretation of results and prepared all the figures.

668

669 **Acknowledgements**

670 The first author's research was supported by the Bundesministerium für Bildung und
671 Forschung (BMBF; German Federal Ministry of Education and Research). The authors
672 acknowledge the colleagues at the Karlsruhe Institute of Technology (KIT) involved in
673 the interdisciplinary virtual institute Dead Sea Research VEnue (DESERVE) for their
674 support and interesting discussions. We acknowledge Sebastian Helgert and Alberto
675 Caldas Alvarez for their assistance in the preparation of the simulations. This article is
676 a contribution to the HyMeX program.

677

678 **References**

679 Alpert, P., and Shay-EL, Y.,: The Moisture Source for the Winter Cyclones in the
680 Eastern Mediterranean. Israel Meteorological Research Papers, 5, 20-27, 1994.

681 Alpert, P., and Coauthors: Relations between climate variability in the Mediterranean
682 region and the tropics: ENSO, South Asian and African monsoons, hurricanes
683 and Saharan dust. Developments in Earth and Environmental Sciences, 4, 149-
684 177, [https://doi.org/10.1016/S1571-9197\(06\)80005-4](https://doi.org/10.1016/S1571-9197(06)80005-4), 2006.

685 Alpert, P., Shafir, H., and Issahary, D.,: Recent Changes in the Climate At the Dead
686 Sea – a Preliminary Study. Climatic Change, 37(3), 513-537,
687 <https://doi.org/10.1023/A:1005330908974>, 1997.

688 Andersson, T., Andersson, M., Jacobsson, C., Nilsson, S.: Thermodynamic
689 indices for forecasting thunderstorms in southern Sweden. Meteorol. Mag.

690 116, 141-146, 1989.

691 Arkin, Y., and Gilat, A.: Dead Sea sinkholes - an ever-developing hazard.
692 Environmental Geology, 39(7), 711-722,
693 <https://doi.org/10.1007/s002540050485>, 2000.

694 Ashbel, D., and Brooks, C.: The influence of the dead sea on the climate of its
695 neighbourhood. Quarterly Journal of the Royal Meteorological Society, 65(280),
696 185-194, <https://doi.org/10.1002/qj.49706528005>, 1939.

697 Ban, N., Schmidli, J., and Schär, C.: Evaluation of the convection-resolving
698 regional climate modeling approach in decade-long simulations, J. Geophys.
699 Res. Atmos., 119, 7889– 7907, <https://doi.org/10.1002/2014JD021478>, 2014.

700 Belachsen, I., Marra, F., Peleg, N., and Morin, E.: Convective rainfall in dry climate:
701 relations with synoptic systems and flash-flood generation in the Dead Sea
702 region. Hydrology and Earth System Sciences Discussions, 21, 5165-5180,
703 <https://doi.org/10.5194/hess-21-5165-2017>, 2017.

704 Böhm, U., and Coauthors: The Climate Version of LM: Brief Description and Long-
705 Term Applications. COSMO Newsletter, 6, 225-235, 2006.

706 Businger, J., Wyngaard, J., Izumi, Y., and Bradley, E.: Flux-Profile Relationships in the
707 Atmospheric Surface Layer. Journal of the Atmospheric Sciences, 28(2), 181-
708 189, [https://doi.org/10.1175/1520-0469\(1971\)028<0181:FPRITA>2.0.CO;2](https://doi.org/10.1175/1520-0469(1971)028<0181:FPRITA>2.0.CO;2),
709 1971.

710 Byun, H., and Kim, D.: Comparing the Effective Drought Index and the Standardized
711 Precipitation Index. Options Méditerranéennes. Séries A. Mediterranean
712 Seminars, 95, 85-89, 2010.

713 Byun, H., and Wilhite, D.: Objective quantification of drought severity and duration. J.
714 Climate, 12(9), 2747-2756, [https://doi.org/10.1175/1520-0442\(1999\)012<2747:OQODSA>2.0.CO;2](https://doi.org/10.1175/1520-0442(1999)012<2747:OQODSA>2.0.CO;2), 1999.

716 Cohen, S., and Stanhill, G.: Contemporary Climate Change in the Jordan Valley. J.
717 Appl. Meteor., 35(7), 1051-1058, [https://doi.org/10.1175/1520-0450\(1996\)035<1051:CCCITJ>2.0.CO;2](https://doi.org/10.1175/1520-0450(1996)035<1051:CCCITJ>2.0.CO;2), 1996.

719 Corsmeier, U., Behrendt, R., Drobinski, P., Kottmeier, C.: The mistral and its
720 effect on air pollution transport and vertical mixing, Atmos. Res., 74, 275–302,
721 <https://doi.org/https://doi.org/10.1016/j.atmosres.2004.04.010>, 2005.

Código de campo cambiado

722 Dayan, U., and Morin, E.: Flash flood – producing rainstorms over the Dead Sea: A
723 review. Geological Society of America, 401(4), 53-62,
724 [https://doi.org/10.1130/2006.2401\(04\)](https://doi.org/10.1130/2006.2401(04)) , 2006.

725 Dayan, U., and Sharon, D.: Meteorological parameters for discriminating between
726 widespread and spotty storms in the Negev. Israel Journal of Earth Sciences,
727 29(4), 253-256, 1980.

728 Dayan, U., Ziv, B., Margalit, A., Morin, E., and Sharon, D.: A severe autumn storm over
729 the middle-east: synoptic and mesoscale convection analysis. Theoretical and
730 Applied Climatology, 69(1-2), 103-122, <https://doi.org/10.1007/s007040170038>,
731 2001.

732 Doms, G., and Baldauf, M.: A Description of the Nonhydrostatic Regional COSMO-
733 Model. Part I: Dynamics and Numerics. Deutscher Wetterdienst, 2015.

734 Doswell, C., and Rasmussen, E.: The Effect of Neglecting the Virtual Temperature
735 Correction on CAPE Calculations. Weather and Forecasting, 9(4), 625-629,
736 [https://doi.org/10.1175/1520-0434\(1994\)009<0625:TEONTV>2.0.CO;2](https://doi.org/10.1175/1520-0434(1994)009<0625:TEONTV>2.0.CO;2), 1994.

737 FAO/IIASA/ISRIC/ISSCAS/JRC.: Harmonized World Soil Database (version 1.2). FAO,
738 Rome, Italy and IIASA, Laxenburg, Austria, (accessed 01.02.2017) , 2009.

739 Fosser, G., Khodayar, S., and Berg, P., 2014: Benefit of convection permitting climate
740 model simulations in the representation of convective precipitation, Clim. Dyn.,
741 44(1–2), 45–60.

742 Gavrieli, I., Bein, A., and Oren, A., 2005: The expected impact of the “Peace Conduit”
743 project (the Red Sea - Dead Sea pipeline) on the Dead Sea. Mitigation and
744 Adaptation Strategies for Global Change, 10(4), 759-777,
745 <https://doi.org/10.1007/s11027-005-5144-z>.

746 European Commission, Joint Research Centre, 2003: Global Land Cover 2000
747 database, (accessed 01.02.2017).

748 GLOBE National Geophysical Data Center, 1999: Global Land One-kilometer Base
749 Elevation (GLOBE) v.1. Hastings, D. and P.K. Dunbar. National Geophysical
750 Data Center, NOAA, (accessed 01.02.2017).

751 Greenbaum, N., Ben-Zvi, A., Haviv, I., and Enzel, Y., 2006: The hydrology and
752 paleohydrology of the Dead Sea tributaries. Geological Society of America,
753 401(4), 63-93, [https://doi.org/10.1130/2006.2401\(05\)](https://doi.org/10.1130/2006.2401(05)).

754 Haylock, M.R., Hofstra, N., Klein Tank, A.M.G., Klok, E.J., Jones, P.D. and New, M.
755 2008, A European daily high-resolution gridded dataset of surface temperature and
756 precipitation. *Journal of Geophysical Research: Atmospheres*, 113, D20119.
757 <https://doi.org/10.1029/2008JD10201>.
758

759 Hochman, A., Mercogliano, P., Alpert, P., Saaroni, H. and Buccignani, E., 2018. High-
760 resolution projection of climate change and extremity over Israel using COSMO-CLM.
761 *International Journal of Climatology*, 38(14), pp.5095-5106.
762

763 Houze, R., 2012: Orographic effects on precipitating clouds. *Reviews of Geophysics*,
764 50(1), <https://doi.org/10.1029/2011RG000365>.

765 Kalthoff, N., Horlacher, V., Corsmeier, U., Volz-Thomas, A., Kolahgar, B., Geiß, H.,
766 Möllmann-Coers, M., and Knaps, A. 2000: Influence of valley winds on transport
767 and dispersion of airborne pollutants in the Freiburg-Schauinsland area, J.
768 *Geophys. Res. Atmos*, 105, 1585–1597, <https://doi.org/10.1029/1999jd900999>.
769

770 Khodayar, S., Kalthoff, N., and Schaedler, G., 2013: The impact of soil moisture
771 variability on seasonal convective precipitation simulations. Part I: validation,
772 feedbacks, and realistic initialisation. *Meteorologische Zeitschrift*, 22(4), 489-505,
773 <https://doi.org/10.1127/0941-2948/2013/0403>.

774 Kunin, P., Alpert, P. and Rostkier-Edelstein, D., 2019. Investigation of sea-
775 breeze/foehn in the Dead Sea valley employing high resolution WRF and observations.
776 *Atmospheric Research*.
777

778 Lensky, N. and Dente, E., 2015. The hydrological processes driving the accelerated
779 Dead Sea level decline in the past decades. *Geological Survey of Israel Report*.
780

781 Llasat, M., and Coauthors, 2010: High-impact floods and flash floods in Mediterranean
782 countries: the FLASH preliminary database. *Advances in Geosciences*, 23, 47-
783 55, <https://doi.org/10.5194/adgeo-23-47-2010>.

784 Metzger, J., Nied, M., Corsmeier, U., Kleffmann, J., and Kottmeier, C., 2017: Dead Sea
785 evaporation by eddy covariance measurements versus aerodynamic, energy
786 budget, Priestley-Taylor, and Penman estimates. *Hydrology and Earth System
787 Sciences Discussions*, 22(2), 1135-1155, [https://doi.org/10.5194/hess-2017-
788 187](https://doi.org/10.5194/hess-2017-187).

789 Miglietta MM, Conte D, Mannarini G, Lacorata G, Rotunno R. 2011. Numerical analysis
790 of a Mediterranean 'hurricane' over south-eastern Italy: sensitivity experiments to sea
791 surface temperature. *Atmos. Res.* **101**: 412–426.
792

793 Moncrieff, M., and Miller, M., 1976: The dynamics and simulation of tropical
794 cumulonimbus and squall lines. *Quarterly Journal of the Royal Meteorological*
795 *Society*, 102(432), 373-394, <https://doi.org/10.1002/qj.49710243208>, 2014.

796 Naor, R., Potchter, O., Shafir, H., and Alpert, P.: An observational study of the
797 summer Mediterranean Sea breeze front penetration into the complex
798 topography of the Jordan Rift Valley, *Theor. Appl. Climatol.*, 127, 275–284,
799 <https://doi.org/10.1007/s00704-015-1635-3>, 2017.

800 Prein, A., Gobiet, A., Suklitsch, M., Truhetz, H., Awan, N., Keuler, K., and Georgievski,
801 G. : Added value of convection permitting seasonal simulations, *Clim.*
802 *Dyn.*, 41(9– 10), 2655– 2677, 2013.

803 Ritter, B., and J.-F. Geleyn, 1992. A comprehensive radiation scheme for numerical
804 weather prediction models with potential applications in climate simulations. *Mon. Wea.*
805 *Rev.*, 120, 303–325.

806 Rostkier-Edelstein, D., Liu, Y., Wu, W., Kunin, P., Givati, A. and Ge, M., 2014. Towards
807 a high-resolution climatology of seasonal precipitation over Israel. *International*
808 *Journal of Climatology*, 34(6), pp.1964-1979.
809

810 Schaedler, G., and Sasse, R.: Analysis of the connection between precipitation and
811 synoptic scale processes in the Eastern Mediterranean using self-organizing maps.
812 *Meteorologische Zeitschrift*, 15(3), 273-278, [https://doi.org/10.1127/0941-](https://doi.org/10.1127/0941-2948/2006/0105)
813 [2948/2006/0105](https://doi.org/10.1127/0941-2948/2006/0105), 2006.

814 Shafir, H., and Alpert, P.: Regional and local climatic effects on the Dead-Sea
815 evaporation. *Climatic Change*, 105(3-4), 455-468,
816 <https://doi.org/10.1007/s10584-010-9892-8>, 2011.

817 Sharon, D., and Kutiel, H.: The distribution of rainfall intensity in Israel, its regional and
818 seasonal variations and its climatological evaluation. *International Journal of*
819 *Climatology*, 6(3), 277-291, <https://doi.org/10.1002/joc.3370060304>, 1986.

820 Smiatek, G., Kunstmann, H., and Heckl, A.: High-resolution climate change simulations
821 for the Jordan River area. *Journal of Geophysical Research*, 116(D16),
822 <https://doi.org/10.1029/2010JD015313>, 2011.

823 Stanhill, G.: Changes in the rate of evaporation from the dead sea. *International*
824 *Journal of Climatology*, 14(4), 465-471,
825 <https://doi.org/10.1002/joc.3370140409>,1994.

826 Vicente-Serrano, S., Beguería, S., López-Moreno, J.: A Multiscalar Drought Index
827 Sensitive to Global Warming: The Standardized Precipitation
828 Evapotranspiration Index. *J. Climate*, 23(7), 1696-1718,
829 <https://doi.org/10.1175/2009JCLI2909.1>, 2010.

830 Vüllers, J., Mayr, G. J., Corsmeier, U., and Kottmeier, C.: Characteristics and
831 evolution of diurnal foehn events in the Dead Sea valley. *Atmos. Chem. Phys.*,
832 18, 18169-18186, <https://doi.org/10.5194/acp-18-18169-2018>, 20, 2018.

833

834 Wernli H, Paulat M, Hagen M, Frei C. SAL – a novel quality measure for the
835 verification of quantitative precipitation forecasts. *Mon. Weather Rev.* 136: 4470–
836 4487, 2008.

837

838 Yatagai, A., Alpert, P. and Xie, P. (2008) Development of a daily gridded precipitation
839 data set for the Middle East. *Advances in Geosciences*, 12, 1–6.

840

841 Yatagai, A., Kamiguchi, K., Arakawa, O., Hamada, A., Yasutomi, N. and Kitoh, A.,
842 2012: APHRODITE: constructing a long-term daily gridded precipitation dataset for
843 Asia based on a dense network of rain gauges. *Bulletin of the American Meteorological*
844 *Society*, 93, 1401–1415.

845

846

847

848

849

850

851

852

853

854

855 **Tables**

	PREC diff _{mn}	REF PMX	SEN PMX	PREC relative diff [%]	Synoptic Situation	REF CAPE _{mx}	SEN CAPE _{mx}	REF KO _{mn}	SEN KO _{mn}	Localised/ Widespread (Subarea affected)
08.12.2004	0,10	30,09	31,31	2,76	ARST	1	1	4,85	4,85	W (A1, A2)
13.01.2006	-0,11	45,64	54,64	-4,26	Cyprus Low	239	225	6,57	6,54	L/W (A1, A3)
16.04.2006	0,11	57,41	56,09	4,89	Syrian Low	43	47	1,97	1,94	L (A1, A4)
10.04.2007	0,29	42,61	70,20	30,78	Cyprus Low	686	679	-4,77	-4,70	L (A2, A4)
13.04.2007	0,12	134,36	127,79	1,62	Cyprus Low	573	576	-1,95	-1,92	L (A1, A2, A3, A4)
12.05.2007	-0,16	41,82	47,90	-8,24	Syrian Low	436	81	-5,30	-5,29	L (A1, A2)
27.01.2008	-0,14	23,11	17,24	-17,25	Syrian Low	7	7	5,12	5,12	W (A1, A3)
25.10.2008	-0,23	139,01	125,73	-16,52	ARST	1274	1361	-5,50	-4,08	L (A3)
13.11.2008	0,30	40,83	45,55	25,68	ARST	25	7	1,37	1,38	L (A2, A4)
14.05.2009	-0,39	59,28	68,84	-8,49	Syrian Low	433	429	-3,90	-3,91	L (A1, A2, A3, A4)
15.05.2009	0,20	49,23	42,28	13,50	Syrian Low	208	203	-2,30	-2,36	L (A1, A2, A3)
31.10.2009	-0,19	166,21	111,79	-7,65	Cyprus Low	435	445	-5,03	-4,46	L (A1, A2)
15.01.2011	0,11	73,02	72,03	3,74	Syrian Low	49	37	7,82	7,83	L/W (A1, A4)
28.05.2011	-0,24	44,51	32,73	-14,33	Cyprus Low	158	170	-10,27	-10,26	W (A2)
14.11.2011	-0,11	42,65	9,34	-65,90	Cyprus Low	2	0	-7,14	-7,12	L (A1, A2)
17.11.2011	0,11	90,07	93,04	4,76	Cyprus Low	386	304	-9,14	-9,16	L (A1)
18.11.2011	-0,11	28,68	34,69	-8,67	Cyprus Low	356	378	-8,61	-8,65	L (A1)
19.11.2011	0,03	58,11	12,36	4,09	Cyprus Low	133	81	-7,60	-7,46	L (A2, A4)
22.10.2012	0,20	29,88	41,64	51,21	ARST	2068	2097	-5,83	-5,59	L (A1, A2)
09.11.2012	-0,11	27,20	22,56	-18,29	Cyprus Low	218	215	3,97	3,98	W (A1)
23.11.2012	-0,21	155,77	117,81	-10,17	ARST	189	286	-2,18	-1,95	L (A1, A2, A3)
25.11.2012	-0,11	41,48	54,33	-7,87	ARST	354	332	4,19	4,37	L (A3, A4)

Con formato: Sangría: Izquierda: 0 cm, Sangría francesa: 1,27 cm

856

857

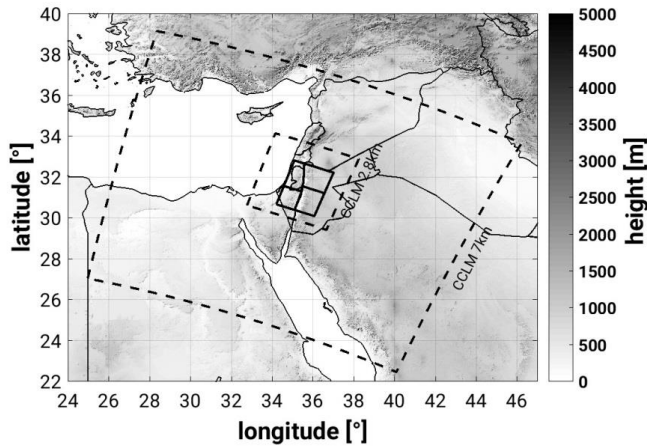
858 **Table 1:** Classification of heavy precipitation cases in the decadal simulation covering
859 the period 2004 to 2013. The areal-mean (study area, Figure 1) difference (PREC_{diffmn})
860 and maximum grid precipitation in the reference (REF_{PMX}) and sensitivity (SEN_{PMX})
861 realizations, the precipitation relative difference in %, the synoptic situation, and the
862 stability conditions illustrated by maximum grid point CAPE (CAPE_{mx}) and minimum
863 grid point KO-index (KO_{mn}) are summarized. Additionally, the nature of the
864 precipitation, localized (L) or widespread (W) and the main subarea affected (following
865 division in Figure 1; A1, A2, A3, A4) are listed.

866

867

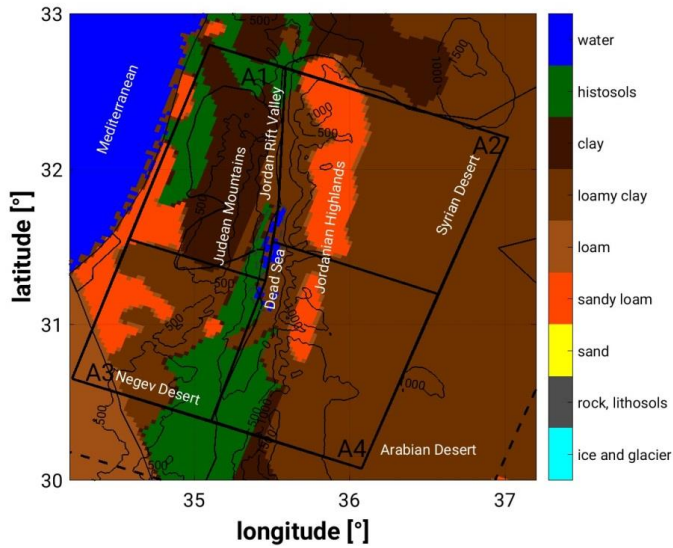
868 **Figures**

869 (a)



870

871 (b)



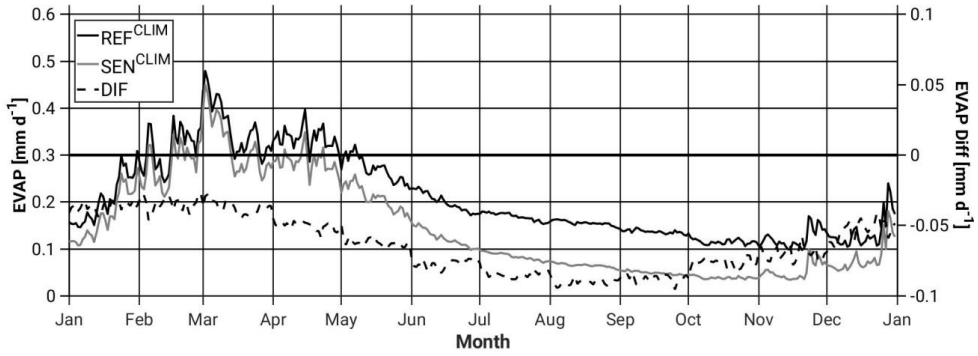
872

873

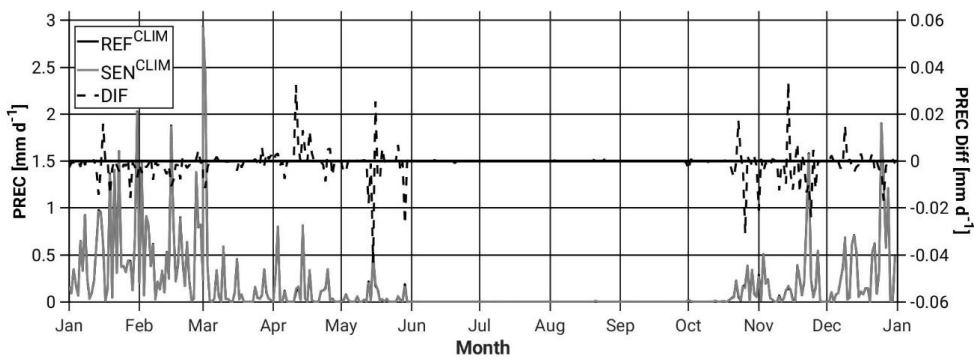
874 Figure 1: (a) Topography (m above msl), simulation domains (dashed lines, CCLM7km
875 and CCLM2.8km) and study area (bold line). (b) Model soil types (colour scale),
876 topography (black isolines) and study area (black bold line) including the 4 subdomains
877 to be examined, A1-4 (Area 1-4).

878 (a)

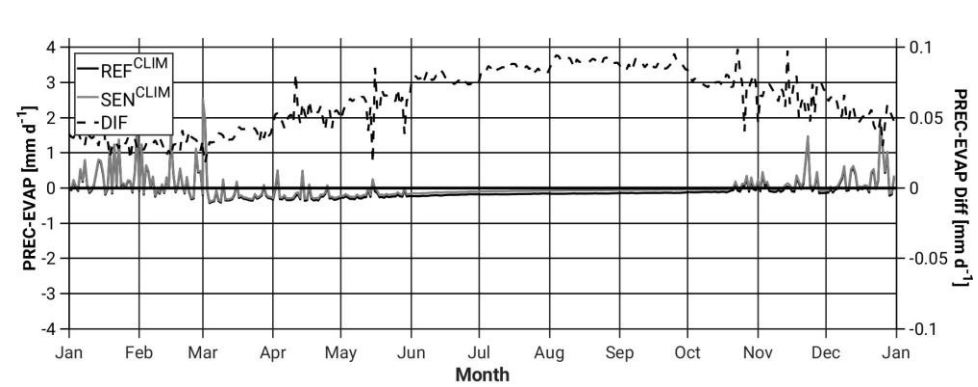
879



880



881



883

884

885

886

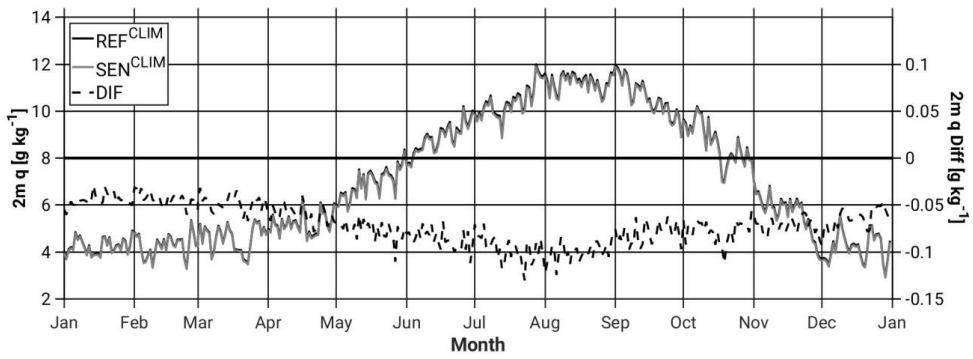
887

888

889

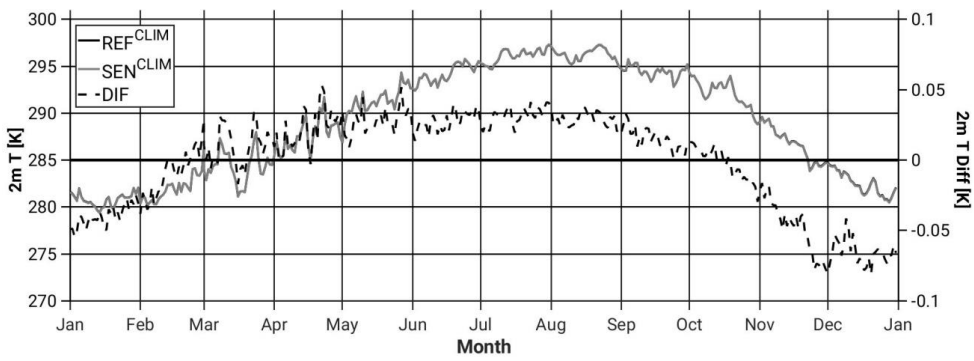
890

891 (b)



892

893



894

895

896

897

898

899

900

901

902

903

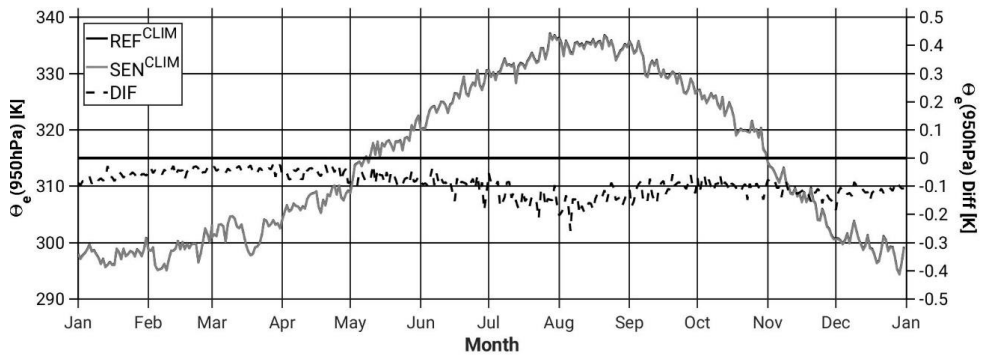
904

905

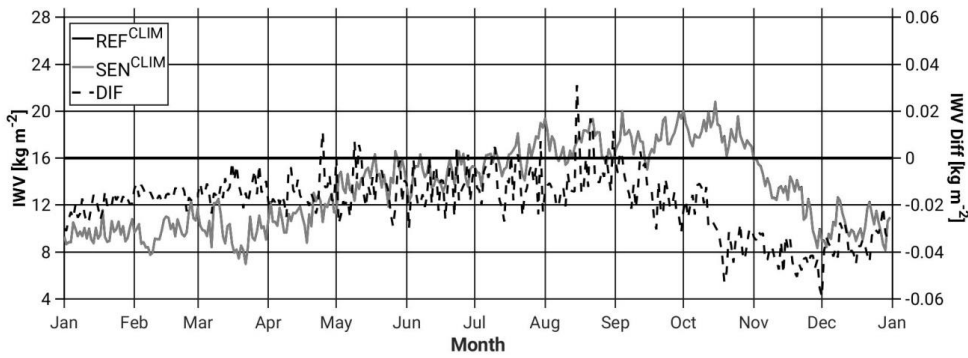
906

907 (c)

908



909



910

911

912

913

914

915

916

917

918

919

920

921

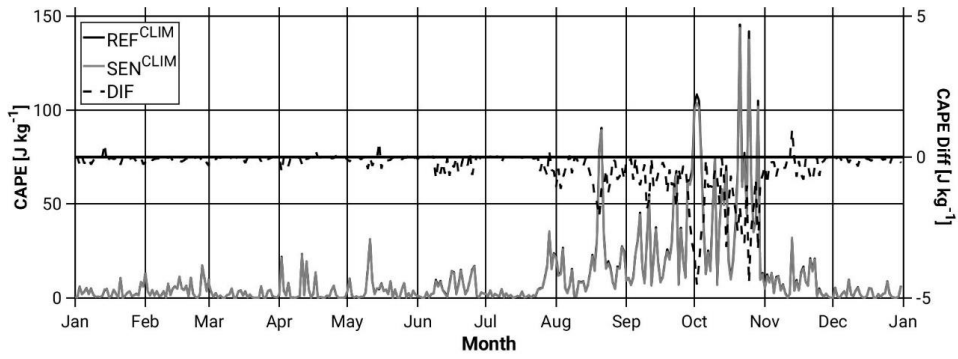
922

923

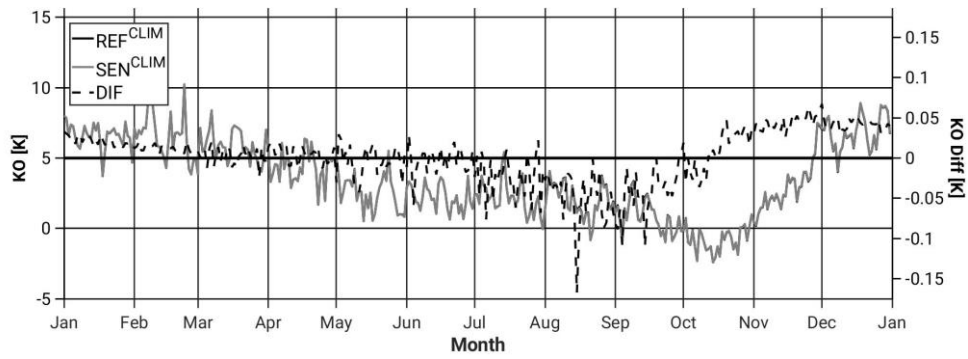
924

925 (d)

926



927



928

929

930

931 Figure 2: Annual cycle of the areal-daily averaged (and differences (black dashed line:
932 SEN-REF)) of (a) evaporation, precipitation, and precipitation minus evaporation (b)
933 specific humidity and temperature at 2-m, and (c) Θ_e below 950 hPa and IWV, and (d)
934 CAPE and KO-index, from the REF^{CLIM} (full black line) and the SEN^{CLIM} (full grey line)
935 simulations. All grid points in the study area (Figure 1) and the period 2004 to 2013 are
936 considered.

937

938

939

940

941

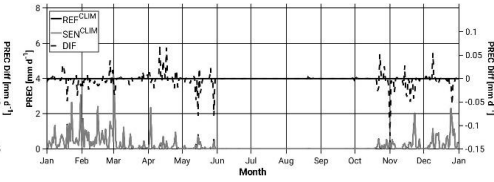
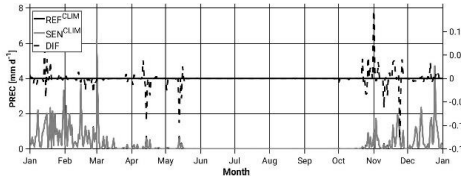
942

943 (a)

944

Area1 (NW)

Area2 (NE)

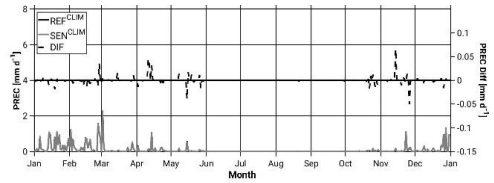
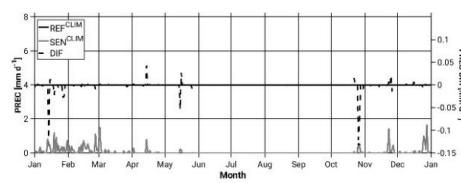


945

946

Area3 (SW)

Area4 (SE)



947

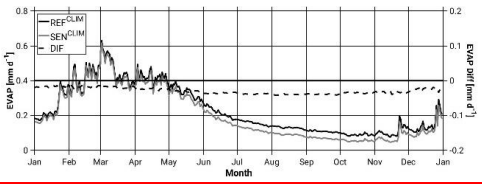
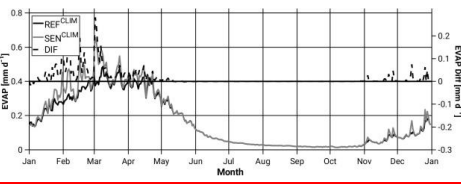
948

(b)

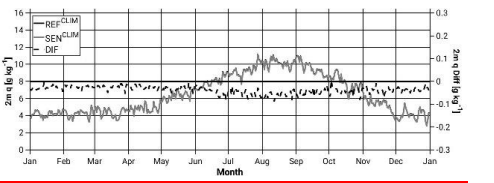
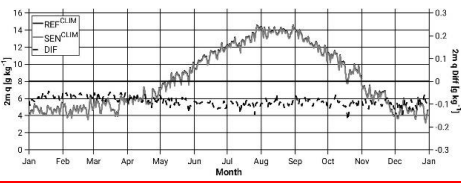
949

Area1 (NW)

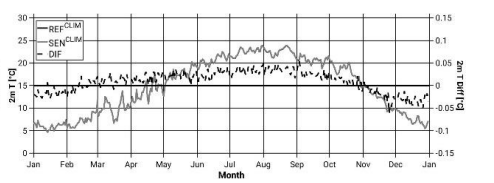
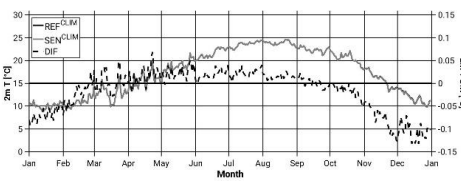
Area2 (NE)



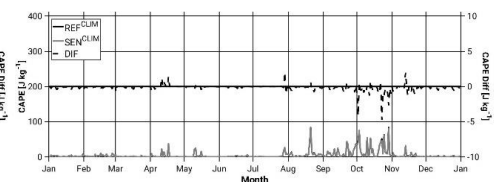
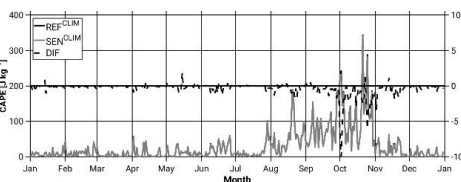
950



951



952



953

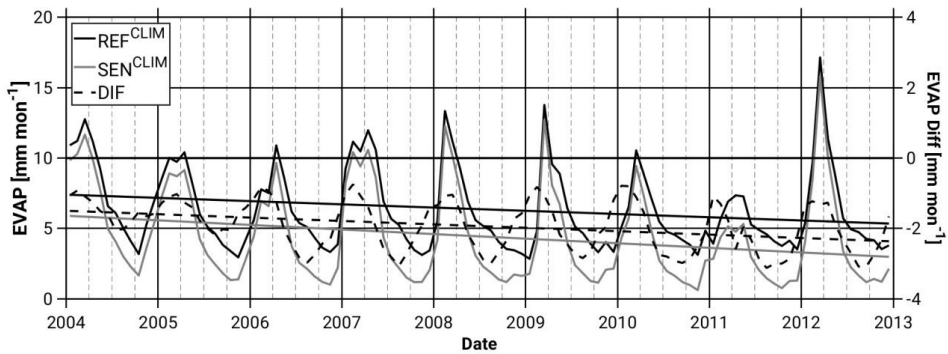
954

955

956 Figure 3: Annual cycle of the areal-daily averaged (and differences (black dashed line:
957 SEN-REF)) of (a) precipitation for areas A1, A2, A3, A4 (see Figure 1b), and (b)
958 evaporation, specific humidity and temperature at 2-m, and CAPE for areas A1 and A2,
959 from the REF^{CLIM} (full black line) and the SEN^{CLIM} (full grey line) simulations. Only land
960 points in the study area (Figure 1) for evaporation, and all grid points for the rest of
961 variables and the period 2004 to 2013 are considered.

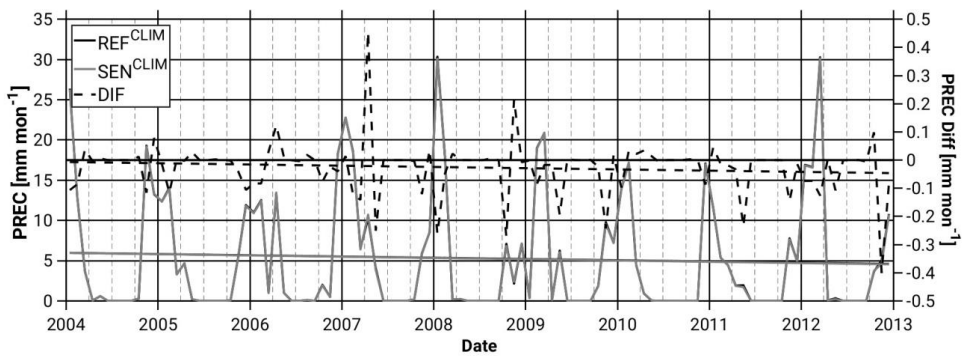
962
963
964
965
966
967
968
969
970
971
972
973
974
975
976
977
978
979
980
981
982
983
984
985
986

987 (a)



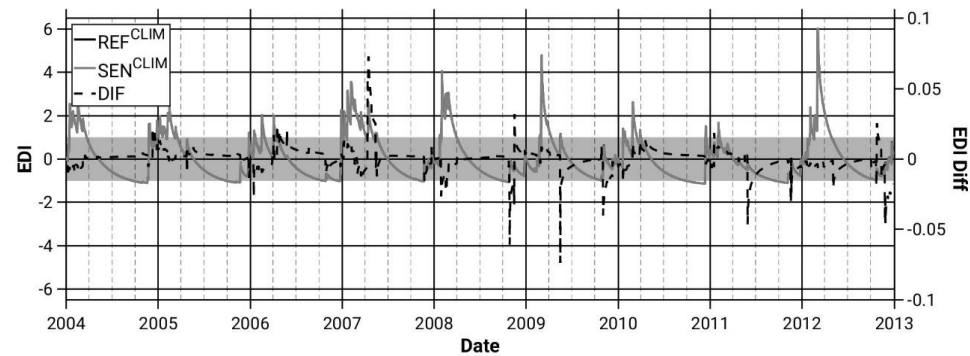
988

989 (b)



990

991 (c)



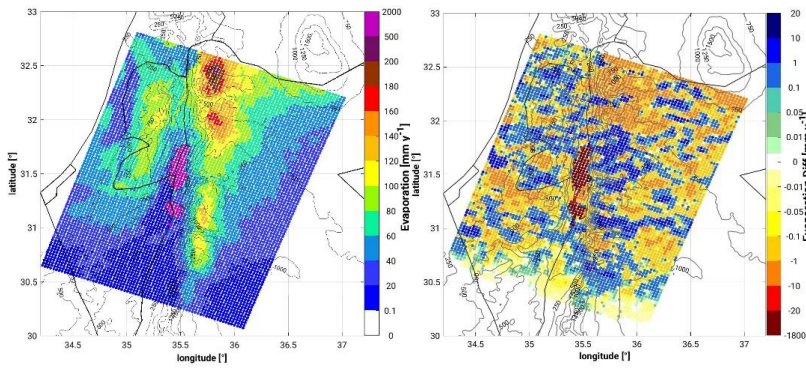
992

993 Figure 4: Temporal evolution of the monthly-daily accumulated areal mean values of
994 (a) Evaporation, (b) Precipitation, (c) Effective Drought Index (EDI), from the REF^{CLIM}
995 (full black line) and the SEN^{CLIM} (full grey line) simulations and differences depicted with
996 black dashed lines. The light grey band in (c) indicates the common soil state (-
997 1<EDI<+1). All grid points in the study area (Figure 1) and the period 2004 to 2013 are
998 considered.

999

1000

1001 (a)

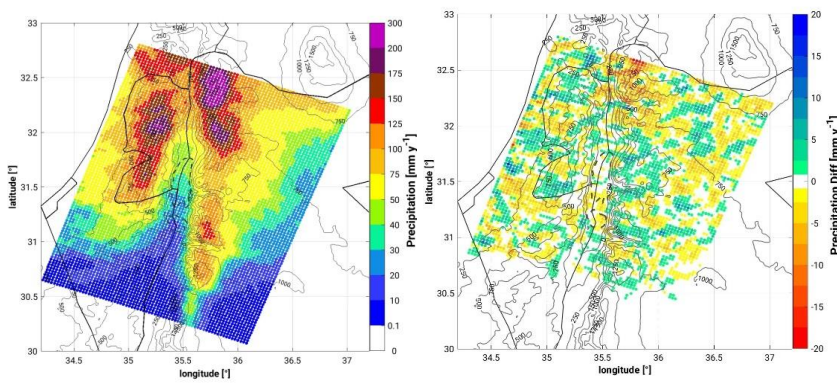


1002

1003

1004

1005 (b)



1006

1007

1008

1009 Figure 5: Spatial distribution of (a) evaporation in the REF^{CLIM} simulation (left) and the
1010 difference between the SEN^{CLIM} and the REF^{CLIM} simulations (right), and (b)
1011 precipitation in the REF^{CLIM} simulation (left) and the difference between the SEN^{CLIM}
1012 and the REF^{CLIM} simulations (right). The period 2004 to 2013 is considered.

1013

1014

1015

1016
1017
1018
1019
1020
1021
1022
1023
1024
1025
1026
1027
1028
1029
1030
1031
1032
1033
1034
1035
1036
1037
1038
1039

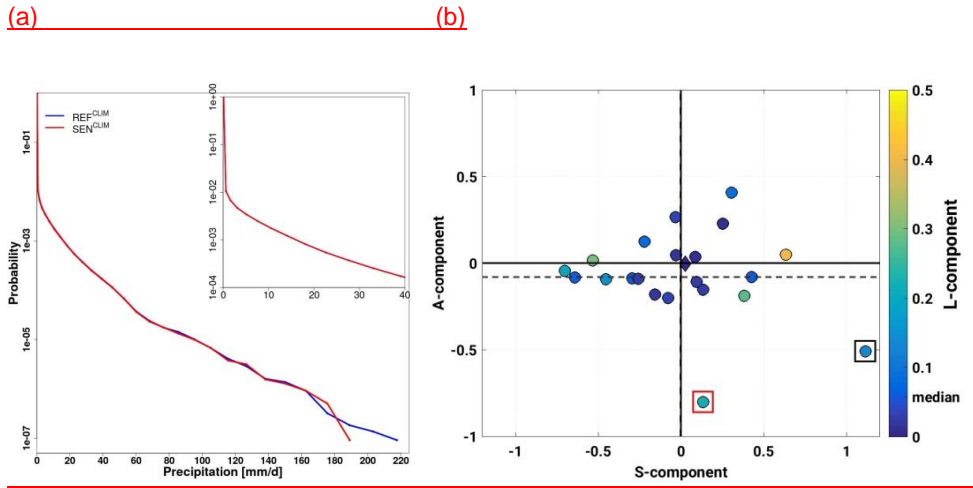
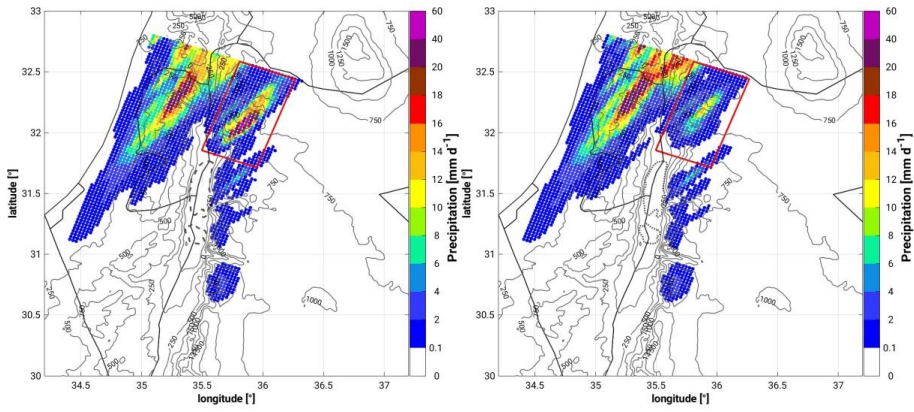


Figure 6: (a) Probability density function of daily precipitation intensities. All grid points in the investigation domain (Figure 1) and the period 2004 to 2013 are considered. (b) SAL diagram between REF^{CLIM} and SEN^{CLIM} simulations. Every circle corresponds to a simulated heavy precipitation event (listed in Table 1). The diamond (close to the zero-zero) illustrates the mean of all events. A-component (amplitude), S-component (structure), L-component (location). The inner colour indicates the L-component. Boxes point out the two events examined in this study, CASE1 and CASE2 (see section 3.2).

1040

1041

(a)

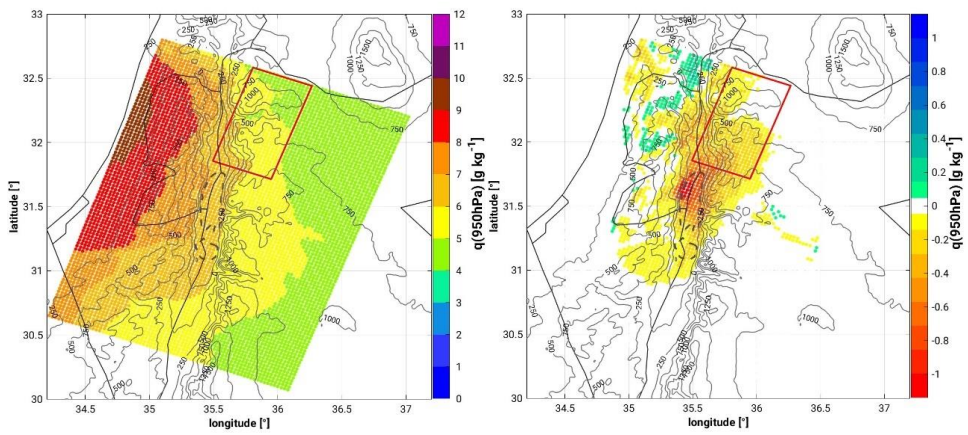


1042

1043

1044

(b)



1045

1046

1047

1048

1049

1050

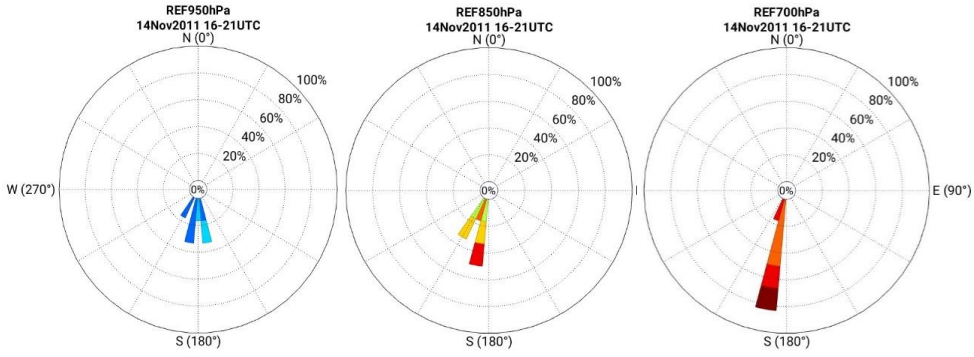
1051

1052

1053

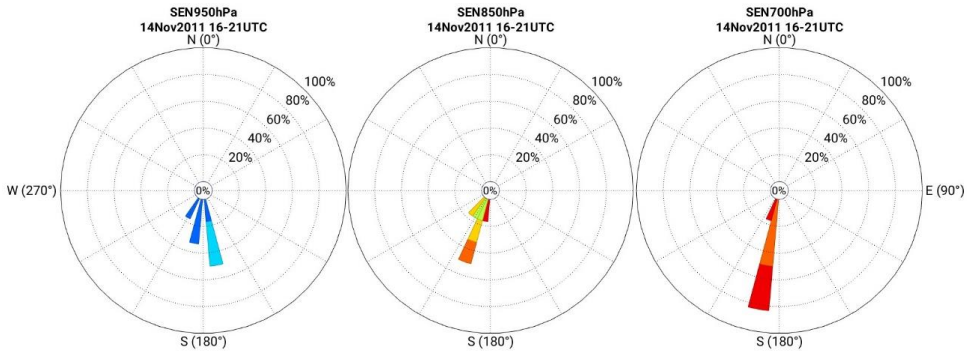
1054

(c)



1055

1056



1057



1058

1059

1060

1061

1062

1063 Figure 7: Spatial distribution of (a) 24-h accumulated precipitation from 14.11 09 UTC
1064 to 15.11 08 UTC from the REF^{14.11} simulation (left) and the SEN^{14.11} simulation (right)
1065 and (b) specific humidity below 950 hPa, from the REF^{14.11} simulation (left) and the
1066 difference between the REF^{14.11} and SEN^{14.11} simulations, as a mean for the 6-h period
1067 prior to convection initiation in the target area (14 November 16 UTC to 21 UTC), and
1068 (c) wind conditions at 700 hPa, 850 hPa, and 950 hPa (no relevant differences with
1069 respect to the 10-m field) for the same time period. Wind roses are centred at about
1070 35.82°E-32.07°N in our target area.

1071

1072

1073

1074

1075

1076

1077

1078

1079

1080

1081

1082

1083

1084

1085

1086

1087

1088

1089

1090

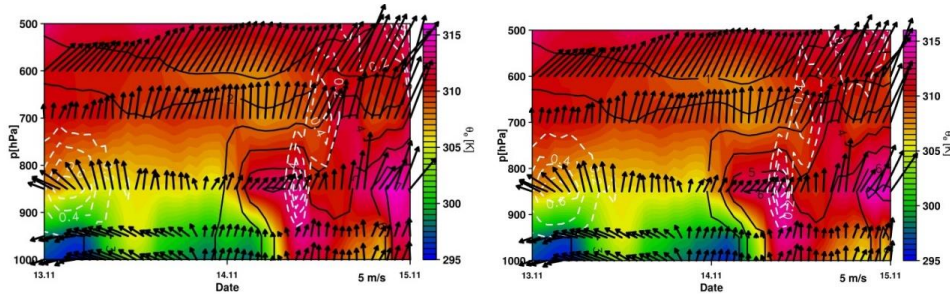
1091

1092

1093

1094

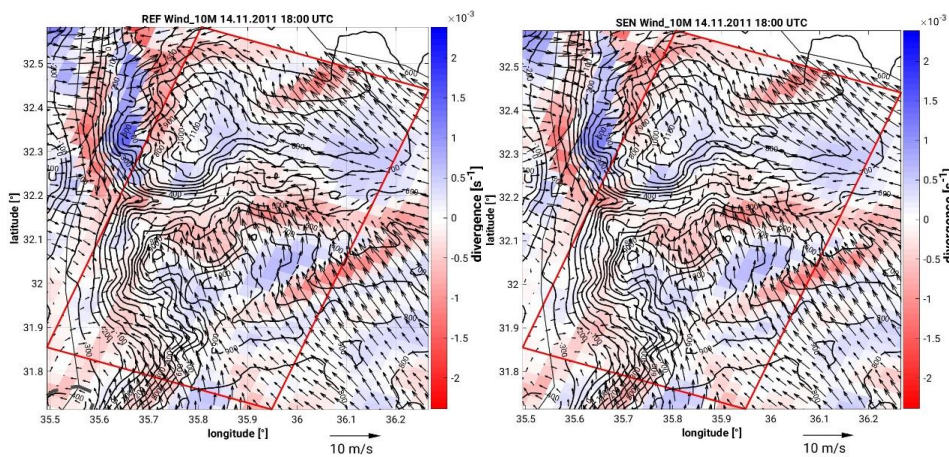
1095 (a)



1096

1097 (b)

1098



1099

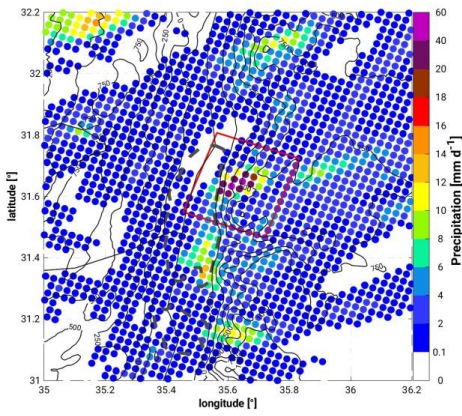
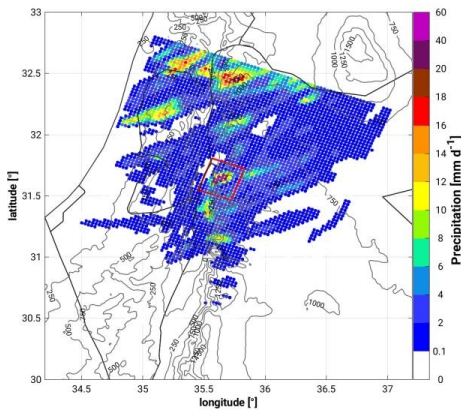
1100

1101 Figure 8: (a) Vertical-temporal cross-section of equivalent potential temperature (colour
1102 scale; K), specific humidity (black isolines; g/kg), horizontal wind vectors (north-pointing
1103 upwards, m/s) and vertical velocity (white dashed contours with 0.1 m/s increments) of
1104 the REF^{14.11} (left) and SEN^{14.11} (right) simulations, over a representative grid point in the
1105 sub-study region, 32.05°N 35.79°E. (b) Spatial distribution of 10-m horizontal wind
1106 (wind vectors; m/s) and corresponding divergence/convergence field (colour scale; s⁻¹)
1107 at 18 UTC on the 14 November 2011 from the REF^{14.11} (left) and SEN^{14.11} (right)
1108 simulations.

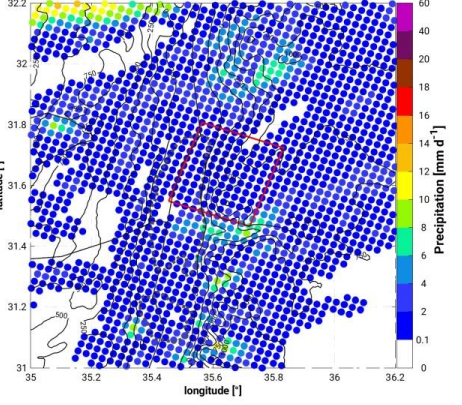
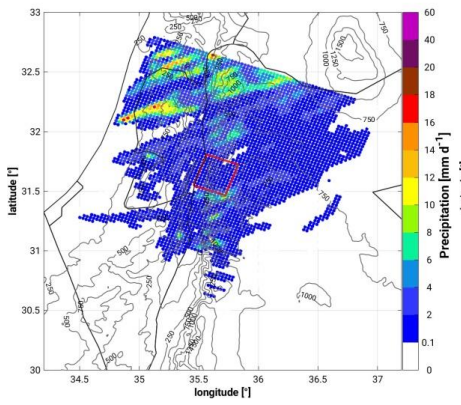
1109

1110

1111



1112
1113



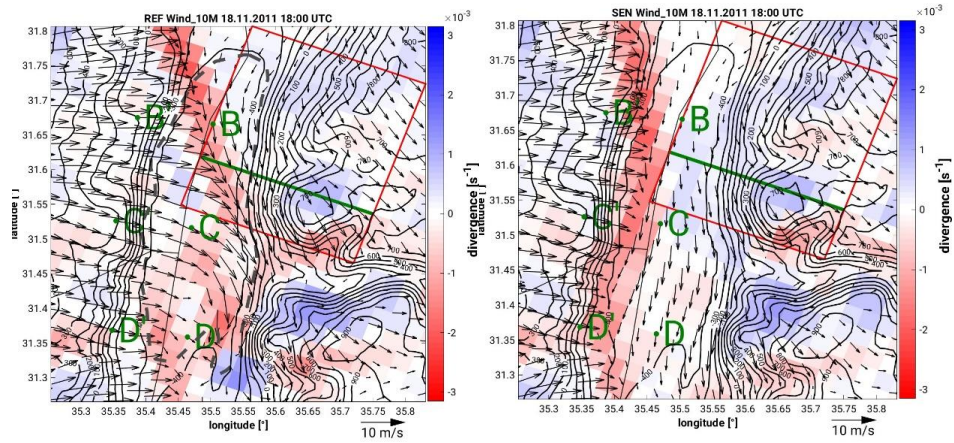
1114
1115
1116
1117

1118 Figure 9: 24-h mean spatial distribution of precipitation from the REF^{19,11} simulation
 1119 (top-left; zoom top-right) and the SEN^{19,11} simulation (bottom-left; zoom bottom-right)
 1120 for the period 18 November 2011 11 UTC to 19 November 2011 10 UTC.

1121
1122
1123
1124
1125
1126
1127

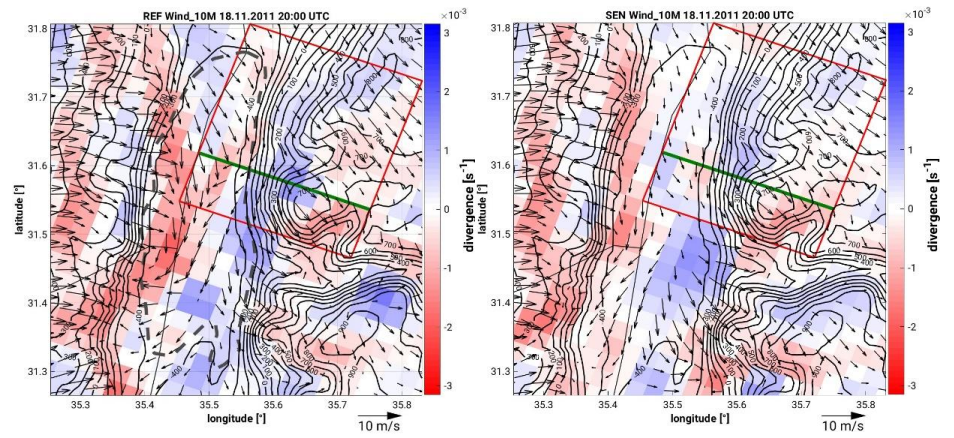
1128

1129 (a)



1130

1131 (b)



1132

1133

1134

1135

1136

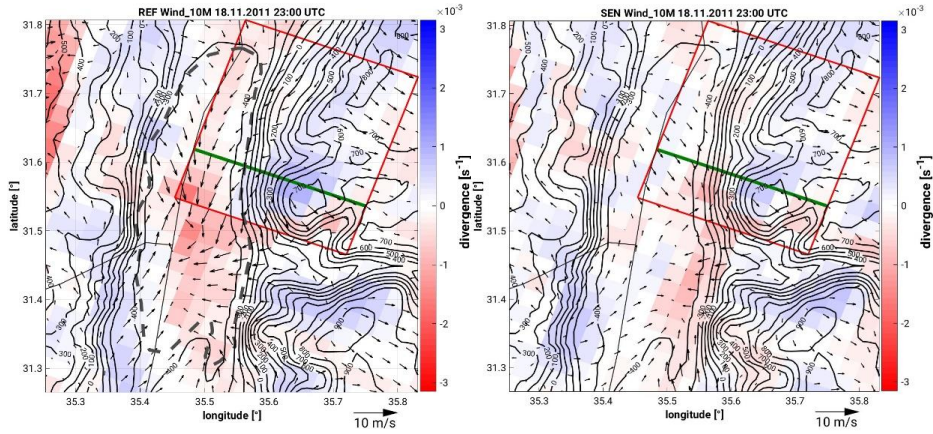
1137

1138

1139

1140

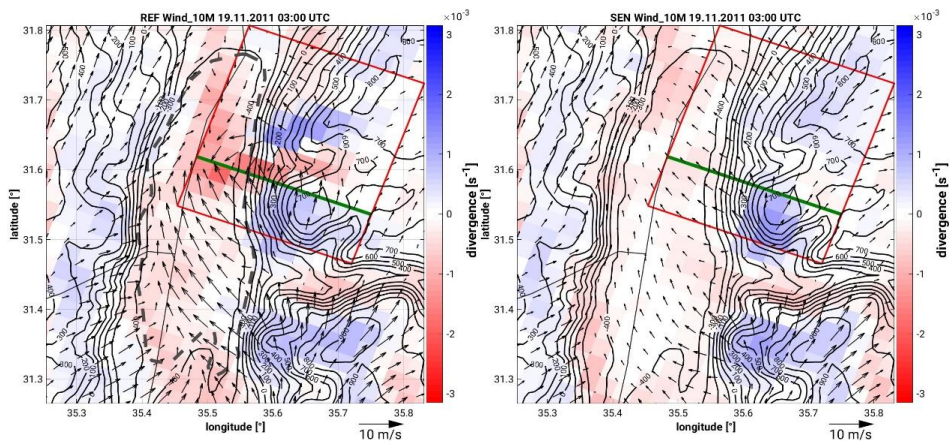
1141 (c)



1142

1143

1144 (d)



1145

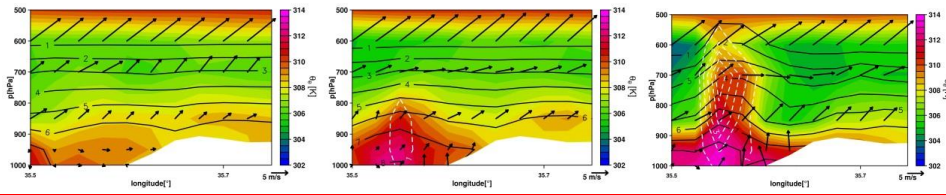
1146

1147 Figure 10: Spatial distribution of 10-m horizontal wind (wind vectors; m/s) and
1148 corresponding divergence/convergence field (colour scale; s⁻¹) at 18 UTC, 20 UTC, 23
1149 UTC on the 19 November, and 03 UTC on the 20 November 2011 from the REF^{19,11}
1150 (left) and SEN^{19,11} (right) simulations. The topography is indicated by the black full
1151 isolines. The transects (B-C-D and B'-C'-D') corresponding to the locations in which
1152 temperature comparisons are made are indicated in Figure 10a. The green line
1153 indicates the position of the vertical cross-section in Figure 11.

1154

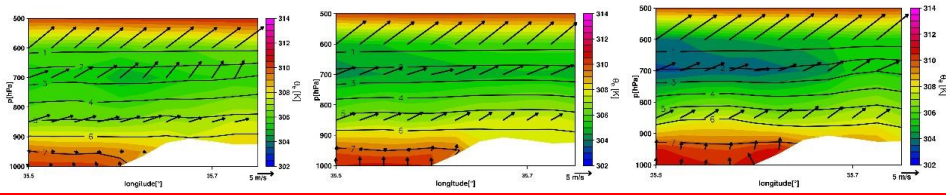
1155

1156



1157

1158



1159

1160

1161

1162 Figure 11: Vertical cross-section of equivalent potential temperature (colour scale; K),
1163 specific humidity (black isolines; g/kg), horizontal wind vectors (north-pointing upwards,
1164 m/s) and vertical velocity (white dashed contours with 1 m/s increments) of the REF^{19,11}
1165 (top) and SEN^{19,11} (bottom) simulations at 01 UTC (left), 02 UTC (middle) and 03 UTC
1166 (right). The location of the cross-section is indicated in Figure 10.

1167

1168

1169

1170

1171

1172

1173

1174

1175

1176

1177